3-10-2013

Self-assembling biomimetic hydrogels with bioadhesive properties for tissue engineering applications

Craig Wiltsey

SELF-ASSEMBLING BIOMIMETIC HYDROGELS WITH BIOADHESIVE PROPERTIES FOR TISSUE ENGINEERING APPLICATIONS

by
Craig Thomas Wiltsey

A Thesis

Submitted to the
Department of Chemical Engineering
College of Engineering
In partial fulfillment of the requirement
For the degree of
Master of Scince in Engineering
at
Rowan University
Dec 19, 2012

Thesis Chair: Jennifer Vernengo

Acknowledgements

First, I would like to thank my family; my mother and father, Tom and Kathy Wiltsey, brothers Colin and Tyler Wiltsey and my fiancé Melissa Allen. Without your love and support I would not have been able to accomplish all that I have in my life, including this thesis!

I would also like to thank Dr. Jennifer Vernengo for her guidance, support and friendship over the past year and a half. I am grateful to Jenn for the opportunity I was given to work on this project and in her lab. I have learned so much from her and hope to apply my newly gained knowledge in the field of biomaterials. Additionally, I would like to thank the members of Dr. Vernengo's clinic project including the present members, Tom Christiani, Jesse Williams, Jake Scaramazza, and Cody Van Sciver and past members Jamie Coulter and Dana Demiduke. I would also like to say thank you to Dr. Cristina Iftode of Biological Sciences and the members of her lab past and present including Katelynn Toomer, Joseph Sheehan, Amanda Branda, Nicholas Albertson, Angelika Nitzl, Sherri English, and Bianca Hess. Without their long hours and commitment to this project the cell work would not have been possible to accomplish. I would like to thank Dr. Mary Staehle for her guidance and support and for graciously agreeing to serve on my thesis committee. Thank you to Dr. Gregory Caputo for the use of his liposome extruder and to Dr. Giuseppe Palmese of Drexel University for the use of his differential scanning calorimeter. Additionally, my gratitude goes out to Marvin Harris and Susan Patterson of the Chemical Engineering department for keeping the project and labs running smoothly

Abstract

Craig Thomas Wiltsey
SELF-ASSEMBLING BIOMIMETIC HYDROGELS WITH BIOADHESIVE PROPERTIES FOR TISSUE ENGINEERING APPLICATIONS
2011/12
Jennifer Vernengo, Ph.D.
Master of Science in Engineering

Tissue engineering is a multidisciplinary field that aims to repair or regenerate lost or damaged tissues and organs in the body. For the repair of certain load-bearing parts of the body, success of a tissue regeneration strategy can be dependent on scaffold adhesion or integration with the surrounding host tissue to prevent dislocation. One such area is the regeneration of the intervertebral disc (IVD). The objective of this work is to generate a bioadhesive polymer that, in addition to bonding with tissue, can support encapsulated cell survival post-adhesion. Thermosensitive poly(N-isopropylacrylamide) (PNIPAAm) was grafted with chondroitin sulfate (CS) (PNIPAAm-g-CS) and blended with aldehyde-modified CS to achieve covalent adhesion upon contact with tissue. Extracellular matrix (ECM) loaded lipid vesicles (liposomes) were incorporated into the copolymer for enhanced cellular biocompatibility. The bioadhesive strength was evaluated in contact with porcine ear cartilage. Additionally, the cytotoxicity of the samples was investigated using a PicoGreen quantitative assay.

Incorporating CS aldehyde into the polymer increased the adhesive strength compared to PNIPAAm-g-CS polymer alone ($p<0.05$), while incorporation of ECM loaded liposomes significantly decreased adhesive strength ($p<0.05$). As lipid concentration increased there were decreasing trends in adhesive strength. Preliminary biocompatibility studies indicate that incorporation of ECM loaded liposomes reduced

cytotoxicity over the copolymer blended with CS aldehyde and no liposomes. Future work will investigate other means of ECM encapsulation to optimize both adhesive strength and biocompatibility.

Table of Contents

Table of Contents (Continued)

List of Figures

List of Figures (Continued)

List of Tables

Chapter 1

Introduction

Lower back pain is one of the most common medical problems world wide and affects nearly 80% of American adults, costing nearly $90 billion annually [1] [2] [3] [4]. The main cause of lower back pain is the degeneration of the intervertebral disc (IVD), resulting from the fall in viable cell population in the nucleus of the IVD and the subsequent inability of the nucleus pulposus (NP) to bear compressive loads [5] [6] [7]. Unfortunately, current treatments for IVD degeneration and lower back pain range from conservative treatments such as medications to more invasive techniques including replacement of the IVD with an artificial disc or fusing the vertebrae [8]. There is a need for a minimally invasive, tissue engineering strategy for repairing and regenerating damaged intervertebral disc tissue.

Tissue engineering is a field that aims to regenerate damaged tissues by incorporating cells into a mechanically stable scaffold [9]. Ideally, a tissue engineering scaffold for repair and replacement of the IVD would overcome the highly invasive nature of current treatments. While a number of tissue-engineered scaffolds have been developed for the IVD, few exhibit the ideal mechanical characteristics to replace native tissue. Additionally, there has been a reported problem of expulsion of implants in the central NP migrating through the damaged annulus fibrosus (AF), making the need for an adhesive scaffold paramount [10] [11].

As with tissue-engineered scaffolds, a number of tissue adhesive components have been investigated. These range from the weakly adhesive but biocompatible fibrin adhesive to strong but poorly biocompatible cyanoacrylate adhesives. In addition, a

number of groups have developed bioadhesive components that show promise for tissue adhesion. These adhesives are comprised chemically modified polysaccharide components, functionalized with aldehyde groups and able to react with the tissue surface via a Schiff's base reaction [12] [13] [14] [15] [16] . Of particular interest are adhesive components made of chondroitin sulfate, a native component of the IVD tissue. Chondroitin sulfate has been modified by a number of researchers to form a novel bioadhesive, however, to our knowledge, has not been incorporated into a tissue engineering scaffold for the repair and regeneration of the IVD [15] [16].

This goal of this work is to develop an adhesive, *in situ* forming hydrogel, capable of supporting encapsulated cells for the tissue engineering of the IVD. To this end, there are three aims of the current work:

Aim 1: Synthesize an adhesive copolymer consisting of poly (N-isopropylacrylamide) graft chondroitin sulfate blended with aldehyde modified chondroitin sulfate and characterize the material properties

Aim 2: Prepare lipid vesicles hydrated with ECM derivatives, verify ECM derivative release, and combine lipid vesicles with the scaffold prepared in Aim 1 and characterize the adhesive properties of the system

Aim 3: Demonstrate the ability of the tissue engineering scaffold to support encapsulated cell survival

In this work, a copolymer scaffold comprised of poly (N-isopropylacrylamide) (PNIPAAm) graft chondroitin sulfate (CS) (PNIPAAm-g-CS) was investigated. The scaffold is comprised mostly of PNIPAAm, allowing it to form *in situ* due to the presense of the lower critical solution temperature (LCST) of PNIPAAm around 29.6°C [17].

Additionally, CS, a native component of the IVD disc tissues allows the scaffold to imbibe water, nutrients, maintain anti-inflammatory characteristics and be susceptible to enzymatic degradation [18] [19]. To provide adhesive properties, aldehyde modified CS (CS aldehyde) was physically blended into the copolymer. The adhesive properties of the adhesive scaffold were investigated as the number of aldehyde groups and weight percentage of CS aldehyde were varied within the system. The overall goal was to develop a system with the maximum adhesive properties.

While CS aldehyde has been investigated as a tissue adhesive, aldehyde groups have been shown to be cytotoxic to encapsulated cells [20] [21]. To combat this effect, lipid vesicles (liposomes) were incorporated into the adhesive scaffold, capable of releasing encapsulated extracellular matrix (ECM) derivatives, gelatin, at body temperature. Gelatin is theorized to be capable of reacting with, or "capping" excess aldehyde groups via the Schiff's base reaction, preventing excess aldehyde groups from being cytotoxic to encapsulated cells. The temperature controlled release is used to ensure that gelatin "capping" does not interfere with the adhesive properties of the system. The release of gelatin from the lipid vesicles and the mechanical properties of the system when liposome concentration was varied were investigated. Finally, the viability of cells seeded within the adhesive copolymer scaffold was tested to determine biocompatibility. Ultimately, this copolymer scaffold has the potential to replace antiquated techniques as a minimally invasive, alternative to highly invasive surgical intervention for the treatment of lower back pain and IVD degeneration.

Chapter 2

Background

2.1 – Spinal Anatomy

The spine can be subdivided into five specific regions, each having different properties and performing slightly different functions. The cervical (neck) region is comprised of 7 vertebrae, each having the smallest vertebral body but with relatively thick IVDs. Traveling down the spine are 12 thoracic vertebrae, each with a slightly larger vertebral body, but with relatively thinner IVDs. In the lower back are the 5 lumbar vertebrae, which are comprised of the largest vertebral bodies and the largest IVDs. The lumbar region is the main load-bearing region of the spine, and therefore is the strongest portion of the spine. Beyond the lumbar are two fused sections with no IVDs, namely the sacrum and the coccyx, with 5 and 4 fused vertebrae respectively [22]. Figure 1 shows the different sections of the spine from both the back and side of the body.

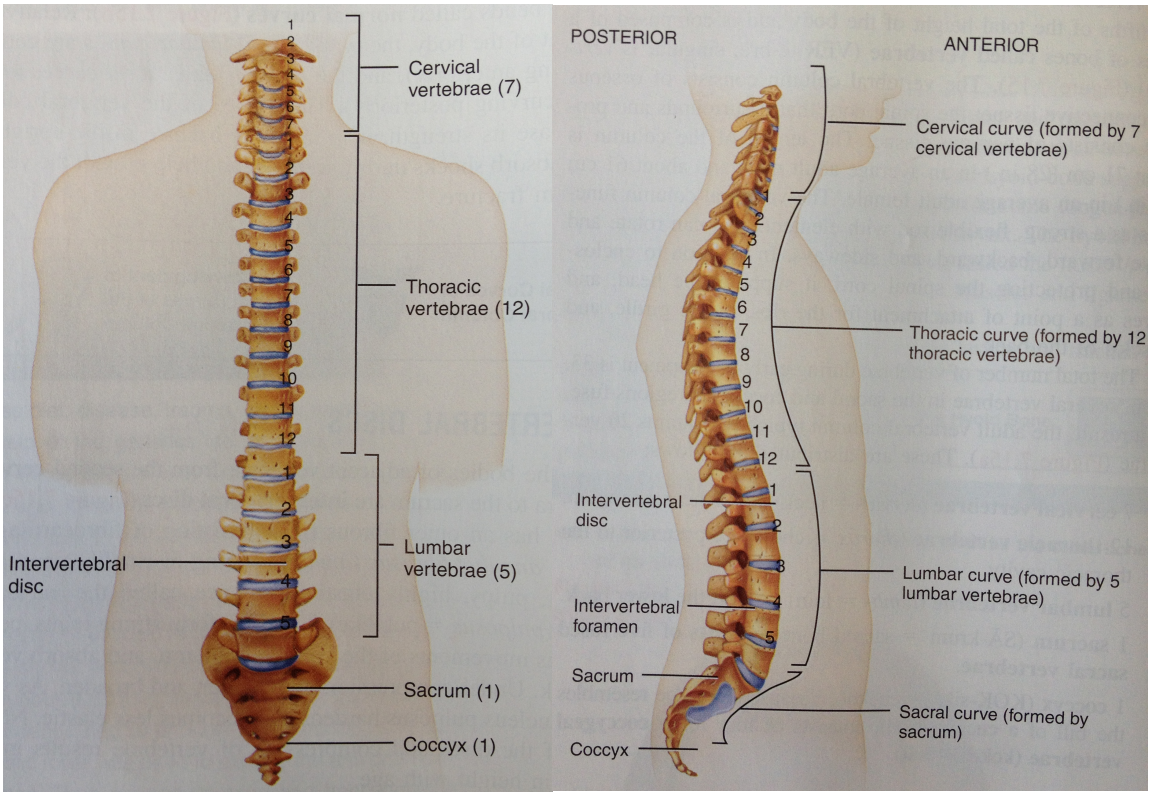

Figure 1: A view of the spine from the back and side, showing the five sections of the spinal column [22]

The spine is comprised of several subcomponents, each performing a specific function. The vertebrae, comprised of bone, provide structure and support. On the anterior side of the vertebrae, facing the inside of the body is the thickest portion of the vertebrae, the vertebral body. The vertebral body is the primary load bearing structure of the vertebrae and therefore must be the thickest part of the vertebrae. Each vertebra also features a small hole, the vertebral foramen, which allows the passage of nervous tissue, blood vessels and additional connective tissues. Additionally, between each vertebra is a collagen and fibrin rich region known as the intervertebral disc (IVD) [22]. Figure 2 shows the placement of the IVD between two vertebrae.

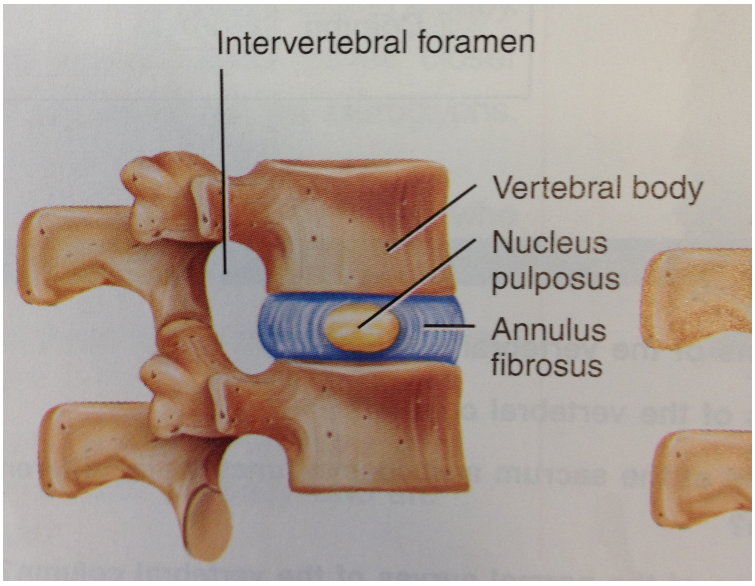

Figure 2: A view of the intervertebral disc showing the body, nucleus pulposus, annulus fibrosus and intervertebral foramen [22]

The IVDs of each region are all slightly different, however their overall composition and structure are consistent in each of the three upper regions of the spine. The IVD has two specific regions, the inner nucleus pulposus (NP) and the outer annulus fibrosus (AF) [22]. The NP can be described as the gel-like region of the IVD located at the center of the disc. The NP is highly hydrated matrix of aggrecan and proteoglycans with embedded collagen and fibrin fibers. The hydrated nature of the NP allows it to maintain pressure and bear compressive forces. Surrounding the NP is the AF, made of collagen fibers arranged in concentric rings or lamellae [23]. The AF itself can consist of approximately 15-25 rings surrounding the NP [24]. The main purpose of each IVD is to

help absorb forces between each vertebrae and to allow the vertebra to move with respect to one another [22].

2.2 – The Intervertebral Disc (IVD)

The intervertebral disc structurally consists of three distinct regions; the inner NP and the outer AF anchored to the vertebral body by two endplates [22]. As previously mentioned, the NP is the gel-like inner core, surrounded by the 15-25 rings, or lamellae, of the AF [24]. The cartilaginous endplate is primarily comprised of hyaline cartilage fibers which run parallel to the vertebral body [23]. The endplate has the highest cell density for any of the three regions of the IVD. Cell density in the vertebral endplate has been estimated to number around 15000 cells/mm^3 [25]. Additionally, the endplate performs two main functions; by providing blood flow to the IVD, the endplate is responsible for providing nutrients to, and removing waste from the intervertebral disc [26].

The annulus fibrosus (AF) is the ring-like structure surrounding the nucleus pulposus (NP) [22]. The cells in the AF are most similar to fibroblasts, although they have been referred to as fibrochondrocytes because of their production of both Type I and II collagen [2] [5]. While the cells produce both Type I and II collagen, the AF is primarily composed of Type I collagen [23]. The Type I collagen produced by the AF cells forms fibers and eventually rings that concentrically surround the NP [24]. The cell density of the AF is lower than the vertebral endplate, with cells numbering around 9000 cells/mm^3 [25].

In the center of the IVD is the nucleus puposus (NP), the gel-like, hydrated central region. The NP is composed of several components including large quantities of

proteoglycans, specifically aggrecan and hyaluronan. Additionally, sulfated glycosaminoglycans (GAGs) including chondroitin sulfate (CS) and keratin sulfate allow the NP tissue to imbibe water and bear compressive loads [23]. The cells of the NP differ from those in the AF, in that they can be described as chondrocyte-like. These cells express markers for chondrocyte-like cells specifically for components like Type II collagen, aggrecan and the mRNA marker Sox-9 [27]. NP cells are chondrocyte-like producing a ratio of proteoglycans to collagen of approximately 27:1 in healthy NP tissue, while in normal cartilage this ratio is approximately 2:1 [28]. Additionally, the cell density in the NP is the lowest of the three IVD regions, with cell densities estimated at approximately 5000 cells/mm^3 [25].

All three IVD components work together allow the spine to bear loads and allowing vertebrae to move freely with respect to one another [22]. The NP and AF specifically work together to absorb loads. The NP is designed to bear compressive loads, bulging outwards and pressing radially on the AF, placing it in circumferential tension [29] [30]. A number of individuals have characterized the native NP and AF tissue in both tension and compression. A summary of the modulus values for the NP and AF in tension and compression can be found in Table 1. It is important to note that the values reported correspond to the function of each tissue; specifically tension values are reported for AF while compressive values are reported for native NP tissue.

Table 1: A summary of the compressive and tensile modulus for native IVD tissue (Adapted from Nerurkar et al [26]**)**

	NP	AF	Reference
Confined Compression	1.0 MPa*	440-750 kPa**	[31]* [32]** [33]** [34]**
Uniaxial Tension (toe/linear)	---	2.5/18-45 MPa	[35] [36] [37] [38] [39] [40] [41]
Biaxial Tension, fixed (toe/linear)	---	9.8/27.2 MPa	[42]

2.3 – Intervertebral Disc Degeneration

2.3.1 – Prevalence and Causes

Lower back pain is one of the most common medical problems, affecting nearly 80% of the adults in the United States at some point in their lifetime and costing approximately $90 billion annually in healthcare costs [1] [2] [3] [4]. More specifically, degenerative disc disease (DDD), which encompasses the spectrum of IVD degeneration problems, affects 12 million individuals in the United States and accounts for approximately $50 billion annually in health care costs [43].

There are a number of factors that can lead to lower back pain and disc degeneration. It has been reported that smoking, intense vibrations and poor nutrient diffusion into the disc tissue can lead to degeneration of healthy disc tissue [44] [45] [46]. Poor nutrient diffusion into disc tissue has been attributed to calcification of the vertebral endplates, which slows the rate of nutrient diffusion into the disc tissue and leading to DDD [47]. As the viable cell population within the disc tissue begins to fall, the metabolic processes within the tissue shift from anabolic to catabolic, further aiding in the degeneration of IVD tissue [5] [6]. Grad et al have called degeneration of the IVD "premature aging" referring to how these processes eventually happen naturally as the

body ages, however appear to be happening earlier than normal in what was once healthy IVD tissue [23].

As the IVD disc ages, there is a decrease in the number of proteoglycans available in the tissue, specifically in the NP of the IVD. The aggrecan within the NP can become fragmented and diffuse from the NP into surrounding tissues [48]. There is evidence that point to catabolic processes, specifically enzymatic degradation of the IVD tissue that leads to the fragmentation of both aggrecan and collagen in the NP. Enzymes families including cathepsins, matrix metalloproteinases (MMPs) and aggrecanases appear to be responsible for the increase in catabolic processes within the IVD [49] [50]. The fall in aggrecan and collagen leads to a decrease in the amount of glycosaminoglycans (GAGs) within the IVD [49]. The GAGs within the NP aid in the intake of water and nutrients into the IVD, therefore a decrease in the GAG population causes dehydration, and subsequently a decrease in the osmotic pressure of the NP [23] [49].

Dehydration of the NP causes a transformation from a gel-like structure to one that is more fibrous, and this affects the ability of the NP to bear compressive loads [7]. The inability of the NP to bear compressive loads places unusual stresses on both the vertebral endplate and AF [51]. These stresses on the vertebral endplate and the AF can lead to bulging and herniation of the IVD. A herniated disc occurs when the inner NP breaks through the lamellae of the AF, penetrating beyond the AF [30]. Examination of herniated IVD show that the NP has migrated through existing tears in the AF, likely due to the extraneous loads placed on the AF from NP dehydration [52]. The herniated IVD placed pressure on the spinal cord, leading to pain and causing an inflammatory response from the body [53] [54].

2.3.2 – Current Treatments

Treatments for lower back pain and DDD can be broken into two categories, conservative treatments and surgical intervention. Conservative treatment involves mitigating the pain caused by degenerated, bulging or herniated IVD. Physical therapy can be used as a non-medicinal route for the treatment of lower back pain. Physical therapies may involve the use of heat and massaging of the area to alleviate some of the pain. If medicinal routes are pursued, the use of anti-inflammatory, analgesic and muscle relaxants may be used to reduce pain in the area. As a minimally invasive conservative treatment, the injection of corticosteroid medication can be used to reduce pain in the area [49] [8].

2.3.2.1 - Discectomy

When conservative treatments have failed, surgical options including lumbar spinal fusion and discectomy can be considered [8]. The prevalence of spinal fusion surgery is reported to be approximately 135.5 cases per 100,000 adults and costs an estimated $82,000 per patient [55]. Discectomy is a procedure that aims to remove one part of the IVD, rather than removal of the entire disc. In discectomy, the part of the IVD that is pressing against the spinal cord, and hence the source of pain, is removed to ease the patient's pain [30]. Although discectomy is able to reduce pain in the short term, the long-term results are more questionable. Bohlman et al report that discectomy has a deleterious affect on the load bearing capabilities of the IVD which ultimately causes the patient's pain to return [56].

2.3.2.2 – Spinal Fusion

A second surgical option for patients who experience pain from DDD is lumbar spinal fusion surgery. Lumbar spinal fusion is a surgery that aims to remove the entire IVD and fuse the two adjacent vertebrae, eliminating movement across that segment of the spine. In addition to the removal of the entire IVD, a bone graft is often used to aid in the fusion of the vertebrae [30]. The goal of spinal fusion is that by removal of the entire IVD and stopping the movement across the joint the patients pain will be eliminated [57]. There is evidence however, that spinal fusion may also not fully alleviate pain in long term studies. A study performed by Lee suggests that both discectomy and spinal fusion accelerate the rate at which degeneration in adjacent IVDs takes place which may cause the patients future pain [58].

2.3.2.3 – Disc Replacement

While spinal fusion seeks to stop pain by removing motion across that segment of spine, others have investigated removing the entire IVD and replacing the disc with a prosthesis that is able to replicate the properties of the native IVD tissue allowing the patient to maintain their mobility of the segment. There are currently two Food and Drug Administration (FDA) approved devices for the total replacement of degenerated IVDs. Namely the prosthetics are the SB Charitè III (DePuy Spine, Raynham, MA) and the ProDisc (Synthes, Inc., Paoli, PA), Figure 3 and Figure 4 respectively [10].

Figure 3: The FDA approved SB Charitè III total disc replacement prosthetic [59]

Figure 4: The FDA approved ProDisc total disc replacement prosthetic [60]

The SB Charitè III has two main parts. The inner core of the prosthetic is a free-floating ultra high molecular weight polyethylene (UHMWPE) oval shaped insert. The core floats between two metallic endplates. The endplates are made of a cobalt-chromium-molybdenum (CoCrMo) alloy. The prosthetic is held in place by twelve teeth (six on each metallic endplate) that anchor the implant to the adjacent intervertebral

bodies. The flat shape of the endplate and the CoCrMo allow is designed to limit the amount of wear and debris from the UHMWPE core [61].

The ProDisc prosthetic is similar in that it too has a UHMWPE, however the core ProDisc is anchored to the lower metallic endplate of the device. Additionally, the ProDisc features a central fin that servers to anchor the device into the adjacent vertebral bodies, compared with the teeth of the SB Charitè III. The fin is designed to promote bone ingrowth into the prosthetic and therefore securely anchor the device to adjacent vertebral bodies [61].

When compared to spinal fusion surgery, the patients who received total disc replacement with a prosthetic device have reported shorter recovery times and lower initial pain [62] [63]. Although prosthetics reported this advantage, there are several problems that occur when total disc replacement is used. Several groups have reported that these prosthetic devices are prone to loosening and possible extrusion [64] [65] [66]. In addition, the polyethylene core of both prosthetic devices is prone to wear and cracking from the stresses experienced between vertebrae. Cracking of the polyethylene core can ultimately lead to the failure of the device, which then must be extracted and replaced [67] [68] [69]. These problems have caused some to question the longevity of such total disc replacement prosthetics [10].

2.3.2.4 – Nucleus Replacement

In addition to total disc replacement surgery, the prosthetic disc nucleus (PDN) (Raymedica, Bloomington, MN) device that is FDA approved for the replacement of the NP alone [10]. The PDN, seen in Figure 5, is used when the AF is still structurally sound, however the inner NP is beginning to degenerate [10] [70]. The PDN makes use of an

inner hydrogel core, covered in a biodegradable mesh that prevents over swelling of the device. The goal of using the PDN is to mimic the natural mechanical properties of native NP tissue [10] [71]. Specifically, a hydrogel is a polymeric material that has the capacity to imbibe water, and remain hydrated in its application, while the polymeric material itself remains intact [72]. The inner hydrogel allows the PDN to maintain a fluid like structure, allowing it to imbibe water, nutrients and function similar to native NP tissue [71].

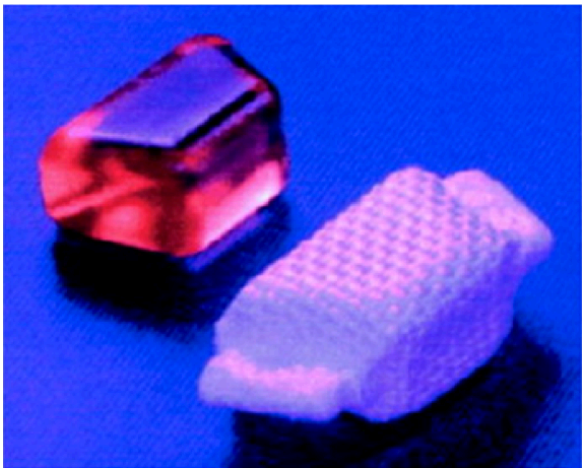

Figure 5: The FDA approved prosthetic disc nucleus (PDN) for the replacement of the NP alone [70]

The advantage to using a prosthetic like the PDN is that the surgery is far less invasive than surgery to remove the entire disc, such as spinal fusion and total disc replacement procedures [73]. Although surgery to implant the PDN is less invasive, it often times damages the AF, which elicits an inflammatory response from the body and can begin the disc degeneration processes, negating the effect of nucleus replacement

altogether [10]. Additionally, several groups have reported that patients who received the PDN experienced problems with device migration and ultimately expulsion from the site of implantation, a problem similar to the other prosthetic devices being used [74] [61].

2.4 – Tissue Engineering

Tissue engineering is a promising area in both biomaterials and NP replacement research. A biomaterial has been defined by D.F. Williams as "material intended to interface with biological systems to evaluate, treat, augment or replace any tissue, organ or function of the body" [75]. Tissue engineering itself makes use of biomaterials integrated with cells with the overall goal being to repair and or regenerate new tissues within the body. The cells synthesize new components, specifically those found in the extracellular matrix (ECM) of the tissue [9]. The ECM components of a tissue are composed of proteins and glycoproteins that can be found in immediate vicinity of the tissue [75]. Of the cells that are used for tissue engineering, the stem cell shows applicability to a wide range of applications because it is found to be both immunologically "invisible" to the patient and can be driven to differentiate into number of different tissues. In the area of IVD repair and replacement, the mesenchymal stem cell (MSC) is particularly important for its ability form bone, muscle and in the case of the IVD, cartilage tissue [9].

The tissue engineer often makes use of a scaffold, or matrix, when repairing tissues. The scaffold is simply the three dimensional biomaterial in which the cells and ECM components are embedded [75]. Lanza, Langer and Vacanti provide a number of properties for the tissue engineering scaffold that provide flexibility to design a system that will accurately replicate the physiological properties of tissues when implanted in the

body. Of these properties, the scaffold can be either permanent (non-biodegradable) or temporary (biodegradable). The scaffold can be designed from a number of materials including synthetic, natural or some combination thereof (semi-synthetic). The scaffold can be designed not only to interact with cells embedded within, but with cells that surround the site of implantation. As such, the scaffold can be designed to release growth factors, proteins and other ECM components that allow for a number of cellular events to occur, including stem cell differentiation and cellular attachment [9].

2.4.1 – Tissue Engineering of the NP and AF

Tissue engineering provides a way to repair and moreover, replace damaged tissues within the body. Of these important areas is the repair and replacement of IVD tissue. Tissue engineering of the AF and NP however proves problematic because of the different cell types and structures found in the AF and NP. While the AF can be described as a fibrochondrocyte, producing primarily type I collagen, the NP remains more chondrocyte like producing primarily type II collagen and a wide variety of GAGs [23] [26] [27]. These differences have made the simultaneous design of a complete IVD difficult and have caused researchers to focus on the replacement of only one component of the IVD rather than both AF and NP.

Several researchers have developed scaffolds for the replacement of the NP based on natural polymers. Among these are polymer scaffolds made of hyaluronic acid (HA). Revell et al replaced the NP with two injectable HA scaffolds (HYAFF 120 and HYADD 3). These scaffolds were able to take the shape of the defect when implanted *in vivo* into a porcine spine. Additionally, the scaffold was embedded with stem cells derived from bone marrow and the scaffold maintained cell viability and promoted the production of

ECM components [76]. Cloyd et al developed HA hydrogels for the replacement of NP tissue and compared the mechanical properties to that of semi-synthetic poly(ethylene glycol) (PEG) grafted chitosan hydrogels and native NP tissue. Cloyd et al found that the hydrogels showed similar properties to that of native NP tissue and therefore would make a good candidate for a NP tissue engineering scaffold [77]. Nesti and Li also developed a HA based scaffold for replacement of the NP. Their HA NP replacement scaffold was enveloped with a biodegradable nano-fiber region that resembles the AF. When embedded with human MSCs *in vitro* for four weeks the cells differentiated into chondrocytes, exhibiting biochemical markers for NP cells. Nesti and Li concluded that this tissue engineered IVD replacement with HA showed promise after *in vitro* testing [78].

Alginate is a second natural scaffold that has been investigated for NP replacement. Chou et al developed a photo-crosslinked alginate matrix for the replacement of the NP. The scaffold was tested both *in vitro* and *in vivo* and shown to produce ECM components indicative of NP cells, specifically in the production of aggrecan and type II collagen. Although the matrix showed more ECM production *in vivo*, a fibrous encapsulation was found to have surrounded the scaffold [79]. Mizuno et al performed trials with a calcium alginate scaffold for NP replacement using athymic mice. The alginate scaffold was seeded with NP cells and then the scaffold was injected into the NP. After 12 weeks this scaffold showed biochemical markers for ECM production including type II collagen, consistent with native NP tissue [80]. A number of other researchers have used alginate scaffolds embedded with cells for replacement of the NP. The cell types included human MSCs, canine and rabbit NP cells and were found to

either form chondrocyte like cells and or begin the production of ECM components that would compare to native NP tissue [81] [82] [83] [84] [85] [86].

Collagen is another natural biomaterial that has been investigated for the repair of the NP. Wilke et al developed a scaffold comprised of type I collagen for the replacement of the NP. Although the material performed successfully when implanted into bovine lumbar vertebrae *in vivo*, the material was not embedded with any cells. Wilke et al also cited problems with expulsion of their polymer when it was tested over longer periods of time [11]. Additional authors have investigated the use of collagen scaffolds, including those combined with HA and human or bovine NP cells to induce ECM production. In these cases ECM production mimicked that of the native IVD tissue, with both type I and II collagen being seen, along with aggrecan and proteoglycans [87] [88] [89]. Halloran et al has also developed an atellocollagen scaffold crosslinked with microbial transglutaminase (mTGase). The scaffold produced similar mechanical integrity and produced ECM components when embedded with bovine NP cells, although excess concentrations of the crosslinking agent adversely affected the viability of cells [90].

Chitosan has been used as another natural scaffold for NP replacement. Roughley et al developed a chitosan based hydrogel for the retention of GAGs and proteoglycans produced by embedded bovine NP cells. The cells were successfully able to produce ECM components when tested *in vitro* and these components were then successfully retained by the chitosan scaffold [91]. Mwale et al also developed chitosan polymers for IVD repair; these injectable polymers included both chitosan chloride and chitosan glutamate crosslinked with genipin. The polymer was tested and proved biocompatibility when injected into mice and was also able to successfully harbor IVD cells. Additionally,

the polymer was injected into cadaver spines and found to completely fill defects in the IVD and was not expelled from the spine [92].

Calcium polyphosphate, another natural polymer, has been investigated construct for the growth and formation of a tissue engineering scaffold for nucleus replacement because of its porous nature. In one study, Séguin et al seeded a calcium polyphosphate scaffold with bovine NP cells and tested for ECM production and mechanical strength *in vitro*. The production of ECM showed components that would be indicative of native NP tissue while the compressive strength of the scaffold was found to be comparable to the native tissue [93]. Hamilton et al investigated the use of calcium polyphosphate for the replacement both the NP and the vertebral end plate. This design was chosen to enhance the integration of the scaffold with the vertebral body. In this study calcium polyphosphate was seeded with bovine NP cells after chondrocytes had deposited a layer of cartilage atop the calcium polyphosphate construct. After 8 weeks, the scaffold formed ECM consistent with native tissues, and the addition of a cartilaginous layer enhanced cellular attachment of the NP cells, ultimately leading to greater ECM production [94].

Combinations of these natural materials have also been investigated in an attempt to create a multicomponent scaffold for the replacement of IVD tissues. Yang et al developed a tri-polymer scaffold for the replacement of the NP and examined these results *in vitro*. The scaffold was comprised of gelatin, chondroitin-6-sulfate and HA and was seeded with human NP cells. Over a four week time period the scaffold maintained cellular viability and showed biochemical markers consistent with native NP tissue [95]. Additionally, Li et al has investigated a multicomponent scaffold made from type II collagen, HA and chondroitin-6-sulfate. This scaffold was enhanced by crosslinked using

both 1-ethyl-3-(3-dimethylaminopropyl)-carbodiimide (EDC) and N-hydroxysuccinimide (NHS). The scaffold was found to exhibit similar properties to the native NP tissue, specifically in that the components chosen for the scaffold itself closely resembled those found in the native tissue [96].

In addition to the natural polymeric materials investigated for IVD tissue engineering, there are a number of synthetic materials that have been examined for their properties and potential to replace the IVD. One such synthetic polymer blend if the polyvinyl alcohol (PVA) and polyvinyl pyrrolidone (PVP) copolymer. Thomas et al developed a PVA-PVP copolymer that was modifiable through freeze/thaw cycles and could be tailored to the properties of the NP. These PVA-PVP hydrogels, when re-swollen, were found to have increasing compressive strength as the amount of dehydration increased. Additionally, through cadaver testing the polymer exhibited comparable compressive strength to native tissues [97]. Joshi et al also developed a PVA-PVP copolymer for the replacement of the NP and tested its mechanical properties. The polymer exhibited comparable properties to native tissue in both confined and unconfined compression testing and cadaver testing [98].

Polyethylene glycol (PEG) is another synthetic hydrogel that could be used for the replacement of the NP. Saldanha et al developed a hydrogel scaffold from PEG for the replacement of NP tissue. The scaffold was embedded with MSCs, and the scaffold was tested for the viability of these cells. This synthetic scaffold was successfully able to promote the viability of MSCs for the replacement of NP tissue [99].

Several researchers have investigated the use of poly (L-lactide-co-glycolide) (PLGA) and poly (L-lactic acid) (PLLA) for NP replacement and ECM production. Ruan

et al developed a scaffold base on PLGA for NP replacement. The scaffold was tested *in vivo* with NP cells. The scaffold was implanted into a canine disc and was able to maintain disc height and stability after implantation and the scaffold also helped to prevent further degeneration of the IVD [100]. Richardson et al developed a scaffold of PLLA to promote the differentiation and viability of human MSCs into chondrocytes. For this study, the MSCs were first differentiated with the transcription factor Sox-9 and then seeded onto the PLLA scaffold. Once embedded in the scaffold the cells maintained their chondrocyte phenotype and produced ECM components including type II collagen and aggrecan, major components of native NP tissue [101].

Among some novel synthetic scaffolds for NP replacement is the use of bioactive glass. Gan et al developed a bioactive glass substrate for the proliferation of rabbit NP cells and subsequent ECM deposition. Researchers have found that the calcium rich region of the bioactive glass aided in cellular attachment and ECM deposition. Additionally, the ECM components produced mimicked those produced by native NP tissue [102].

While there have been many advances in tissue engineering of the IVD, a number of researchers have expressed problems with expulsion from the area and migration of the implants. This is especially prevalent with this scaffolds that are able to be injected into the area and cure *in situ* making the need for a tissue adhesive used in conjunction with tissue engineering scaffolds a paramount concern for biomedical engineers [10] [11].

2.4.2 – Poly (N-isopropyl acrylamide) for Tissue Engineering Applications

One of the most interesting polymeric materials currently under investigation for tissue engineering applications is poly (N-isopropyl acrylamide) (PNIPAAm), shown in Figure 6. Many hydrocarbons experience a lower critical solution temperature (LCST), the lowest temperature in which the polymer and the solvent are miscible in one another. PNIPAAm, unlike other hydrocarbons, is susceptible to a temperature dependent phase transition that occurs between 31-32°C, the reported LCST of PNIPAAm [17]. Below its LCST, PNIPAAm forms a number of hydrogen bonds with water. As the temperature is increased above the LCST, these hydrogen bonds are broken as the polymer under goes a conformational change, ultimately leading to its decreased miscibility in water [103]. Undergoing this conformational change, PNIPAAm begins to form more hydrophobic interactions with the polymer side chain groups. These interactions cause the PNIPAAm polymer chains to aggregate into a single mass, thereby "self-assembling" into the hydrogel state [17]. Because this phase transition happens above the LCST temperature of 32°C, PNIPAAm is an excellent scaffold for use in a number of tissue engineering applications within the body for its ability to be implanted minimally invasively and subsequently self assemble at body temperature.

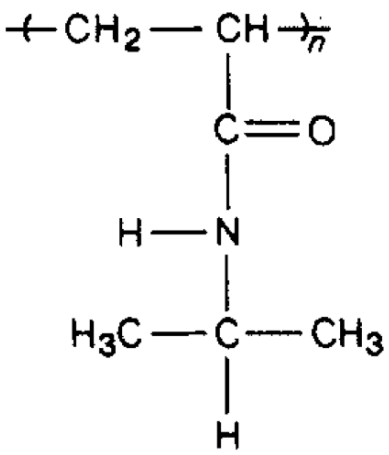

Figure 6: PNIPAAm molecular structure [17]

PNIPAAm has been used in a number of broad tissue engineering applications. Akiyama et al developed a PNIPAAm copolymer scaffold including polystyrene (PS) for cellular attachment. Attachment of the cells was controlled by temperature, where at high temperatures with the PNIPAAm-PS hydrogel was self-assembled the cells would remain attached and when the polymer was dropped below its LCST, the cells would detach from the scaffold [104]. Kim and Healy developed a PNIPAAm scaffold with acrylic acid (AAc) for tissue engineering applications. This scaffold contained a peptide sequence recognizable by MMPs while allowed for enzymatic degradation and have minimal affect on the thermosensitve response of the polymer at its LCST [105]. In addition, Ohya et al developed a PNIPAAm-HA scaffold for various tissue engineering applications. This scaffold was found to inhibit the attachment of cells when it was used as a coating on surfaces, although this was likely due to hydrophobic interactions from the side chains of HA [106].

In addition to general tissue engineering applications, a number of researchers have developed PNIPAAm based scaffold for the repair of cartilaginous tissues. Chen et al developed a PNIPAAm-chitosan scaffold for the replacement and repair of cartilage, specifically the meniscus. The introduction of chitosan allowed for increased mechanical properties over the homopolymer. Testing *in vivo* showed that the scaffold was non-cytotoxic and demonstrated the ability to maintain cellular viability [107]. Stile et al examined PNIPAAm and PNIPAAm-AAc scaffold for cartilage tissue engineering. When this scaffold was embedded with bovine chondrocytes it promoted both proliferation and cellular viability for four weeks *in vitro*. The authors mention that this polymer could be outfitted with enzymatically degradable crosslinks and that the polymer demonstrated promising biocompatibility in preliminary *in vivo* studies [108].

In the area of the spine, researchers have investigated the use of PNIPAAm based scaffolds for the repair of spinal cord injuries. Comolli et al investigated a PNIPAAm-PEG scaffold for repairing spinal cord injuries. Again, the scaffold was easily tailored to be applicable for number of applications and had the ability to release bioactive trophic factors for a four-week period at physiological conditions. Additionally, this scaffold promoted the attachment and proliferation of MSCs within [109]. Conova et al developed both a PNIPAAm-g-PEG and PNIPAAm-g-methylcellulose (MC) scaffold for spinal cord repair. The scaffold was tested *in vivo* using rats and found to completely fill the defect when injected. The PNIPAAm-PEG scaffold was found to support cell proliferation when tested *in vivo*, and while the PNIPAAm-MC scaffold was not tested *in vivo*, it was expected to perform similarly. Additionally, this scaffold was able to

successfully deliver neurotropic factors, a key component to the regeneration of axons in the spinal cord [110].

Few researchers have investigated the use of PNIPAAm for the repair and regeneration of damaged IVDs. Vernengo et al developed an injectable PNIPAAm-PEG scaffold for the repair of NP tissue. With the addition of PEG to this polymer, it was able to imbibe more water than the homopolymer. When the polymer was allowed to swell for 60 days it exhibited mechanical properties that were similar to those of native disc tissues [111]. The authors of this study also incorporated poly (ethylene imine) (PEI) into the polymer. Once the polymer was injected into the defect, an injection of gluteraldehyde was administered to prevent expulsion of the implant. This adhesive works via aldehyde-amine chemistry, which has applications in a number of different tissue engineering areas [112].

2.5 – Bioadhesives

2.5.1 – Bioadhesive Overview

Bioadhesives are of specific interest to the tissue engineer for a variety of applications. Specifically, a bioadhesive is any component that is used in a medical application for the purposes of adhering two tissues together [75]. The field bioadhesive is so broad that it encompasses many materials, and like biomaterials, can be natural, synthetic or some combination thereof.

2.5.2 – Cyanoacrylates

One widely used synthetic bioadhesive is the cyanoacrylate adhesive, seen below in the varying forms available as Figure 7. Cyanoacrylate adhesives are widely used in medical applications for wound closure, however they have found some use in surgical

applications, specifically hemostasis and fistula repairs [113] [114]. In addition to these surgical applications, Pollak and White performed a review of the use of cyanoacrylate adhesives and their use for embolization within the body [115].

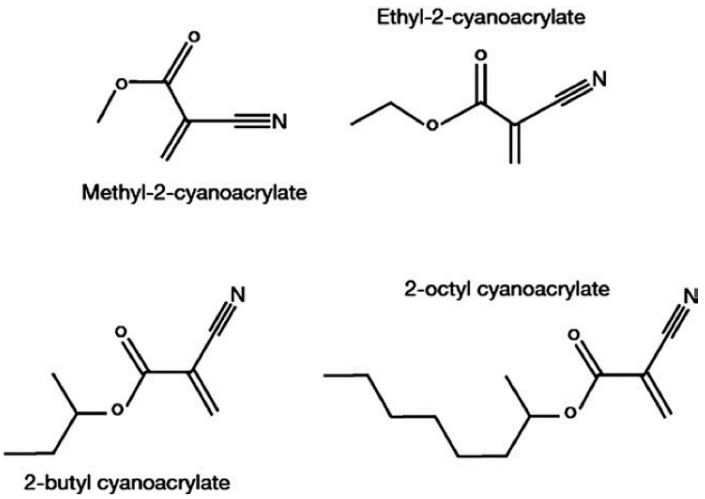

Figure 7: A variety of the commercially available cyanoacrylate bioadhesives [116]

A number of authors have investigated the use of cyanoacrylate adhesives for an number of different applications. Toriumi et al investigated the use of cyanoacrylate adhesives for attaching different grafts within the body, and examined how the chain length of the adhesive affected the histology of cells. The authors examined attaching a bone graft to the cartilage of rabbit ears with both ethyl-2-cyanoacrylate (Krazy Glue) and butyl-2-cyanoacrylate (Histoacryl). The authors found that the longer (butyl) cyanoacrylate adhesives have a decreased inflammatory and foreign body response from cells in addition to being less toxic to tissues [117]. The shorter (methyl and ethyl)

cyanoacrylates are potentially toxic because of their quick degradation into harmful byproducts, including formaldehyde [118].

Ekelund and Nilsson examined the use of cyanoacrylate adhesives and their possible use in healing bone fractures. This study found that the use of cyanoacrylate adhesives causes a severe inflammatory response from the body, and its slow degradation rate caused it to remain within the body weeks after use. When the authors tested the use of the adhesive *in vivo* they found that in some instances the adhesive can completely inhibit the formation of new bone [119]. In addition to bone repair, the use of cyanoacrylates for repairing cartilage has also been examined. Reckers et al investigated the use of cyanoacrylates for repair of the meniscus *in vivo* with rabbits. The cyanoacrylates had such a negative effect, including severe inflammatory responses and tissue necrosis, that it caused the early termination of experimentation [120].

There are several advantages to the use of cyanoacrylate adhesives; cyanoacrylates are a strong adhesive with strength on the order of 1000 kPa and they have markedly faster sealing times than other commercially available adhesives, specifically fibrin glue [121] [122]. While these advantages make cyanoacrylates an attractive choice, they have several severe disadvantages that make their use very limited. Cyanoacrylates have two main toxic degradation, cyanoacetate and formaldehyde, which while not a problem for external wound closure, may cause a problem in other internal application. While the rate of the degradation can be controlled by chain length, the longer the side chains the slower the degradation, all cyanoacrylates form these two byproducts [116]. The polymerization of cyanoacrylates, allowing the adhesion to take place, forms via an exothermic reaction which can damage tissues and cause burns [123].

Finally, cyanoacrylate adhesives have been associated with severe tissue necrosis when tested *in vivo* which is possibly attributed to the oxidation and ultimate lysis of cell walls [124]. While cyanoacrylates have superior strength over other adhesives, their poor biocompatibility limits their use in many applications.

2.5.3 – Fibrin Adhesives

Fibrin adhesives represent a group of natural adhesives and is comprised of fibrinogen and thrombin. The two components of the fibrin adhesive are mixed at the site of adhesion and the adhesive mimics the final stages of the blood clotting cascade [125]. The current applications for fibrin adhesives are similar to those of cyanoacrylate adhesives including uses for wound closure. Fibrin adhesives are also used for a number of surgical applications including hemostasis and tissue adhesion [114].

As with cyanoacrylate adhesives, a number of authors have investigated alternative uses for fibrin adhesives. In comparison with the cyanoacrylate adhesive for meniscus repair, Reckers et al investigated the use of fibrin *in vivo* using rabbits. The rabbits treated with fibrin adhesives had scores for inflammatory response, fever, distance walked, diet refusal and knee extension comparable to meniscuses that were secured using sutures. Although this was comparable, the authors found that the fibrin adhesives impaired the spread of cells changing the appearance of the meniscus over knees secured with sutures [120]. Brittberg et al also examined the use of fibrin adhesives for the repair of cartilage using rabbit knees. These authors found that the adhesive was a poor scaffold *in vivo* unable to promote cell proliferation and the adhesive was insufficient to fill large defects in the cartilage. Additionally, the adhesive performed much more poorly than if the defect had been sutured shut [126].

A number of authors have investigated the development of fibrin adhesive scaffolds for tissue engineering applications. Bensaïd et al developed a scaffold consisting of fibrin adhesive that could be used to deliver human MSCs. This scaffold successfully promoted the growth and proliferation of human MSCs, however when implanted into mice, the cells migrated beyond the scaffolding. This indicated that this fibrin scaffold would perform better as a delivery vehicle for cells [127]. Christman et al examined a fibrin scaffold for the treatment of myocardial infraction. This scaffolding supported myoblast cell growth and proliferation *in vitro*. In addition, when the cells were transplanted into rats using the fibrin adhesive the viability of the cells and blood flow to the area were both increased [128]. Yamada et al also developed a fibrin scaffold, including β-tricalcium phosphate, to encapsulated MSCs for bone repair and regeneration. The fibrin adhesive was shown to promote the viability and proliferation of MSCs and produced bone only when the β-tricalcium phosphate was included into the mixture. After 8 weeks *in vivo* using rats, the scaffold successfully produced bone tissue [129]. Similarly, Lee et al showed that fibrin adhesive combined with macroporous biphasic calcium phosphate and rat MSCs successfully promoted bone growth [130].

While the biocompatibility, namely the cell encapsulation ability, of fibrin adhesive is an advantage over cyanoacrylate adhesives; fibrin adhesives have relatively poor strength. Chivers and Wolowacz showed that the strength of cyanoacrylate adhesives is approximately 200 times stronger than joints sealed with fibrin adhesive [121]. A comparison of these adhesive strengths can be seen in Table 2.

Table 2: Relative adhesive strength of cyanoacrylate adhesive and fibrin adhesive adhered to cartilage in both lap and butt joints [121]

	Cyanoacrylate	Fibrin
Butt Joint Strength (kPa)	1000	4.9
Lap Joint Strength (kPa)	700	---

2.5.4 – Aldehyde Based Adhesives

In addition to the two commonly used adhesives, fibrin and cyanoacrylates, there are a number of innovative aldehyde based adhesives developed that are able to react with tissues via a Schiff's Base reaction. A Schiff's base reaction takes place between aldehyde groups on the adhesive and amines located on the tissue surface, forming one covalent bond and the production of water, seen below as Equation 1 [131].

Equation 1: A Schiff's base reaction between aldehyde groups on the adhesive and amines on tissues, producing water and a covalent bond [131]

$$-CHO + H_2N - \rightarrow H_2O + -CH = N -$$

One aldehyde adhesive currently in use is the glutaraldehyde adhesive (produced under the trade name BioGlue) seen in Figure 8. BioGlue is an injectable adhesive consisting of two components, specifically bovine serum albumin (BSA) and glutaraldehyde. Currently, BioGlue is approved by the FDA for the repair of larger blood vessels (i.e. aorta) and hemostasis [132]. The limited area of use is because the long term effects of BioGlue on the body are not well understood and require further investigation [133].

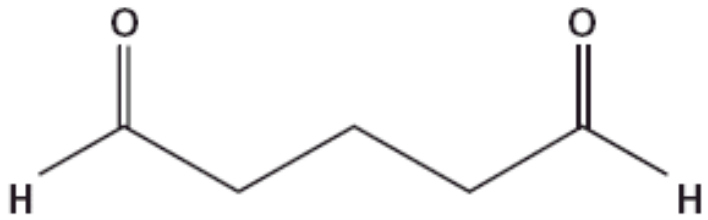

Figure 8: Glutaraldehyde, the adhesive component of the commercially produced BioGlue [134]

Several researchers have investigated the use of glutaraldehyde adhesives in applications outside of what is currently approved. Kilmo et al performed a clinical trial using BioGlue to seal surgical wounds in the area of the cranium and spinal cord. The use of BioGlue in this area was found to cause a severe inflammatory responses and complications, causing the authors to discourage the use of BioGlue in these applications [135]. Gaberel et al retrospectively studied patients who underwent craniotomies where BioGlue was used as the sealant. The authors here linked the use of BioGlue to increased likelihood of surgical site infection, likely due to the inflammatory response to the adhesive [136]. Hidas et al performed a clinical trial in the use of BioGlue for renal surgeries. The authors found that in this case, BioGlue successfully reduced both the amount of blood lost, thereby decreasing the need for transfusions, and reduced the prevalence of urinary fistula formation. These results were found to be comparable to the traditional suturing technique [137].

In addition to the clinical trials, Fürst and Banerjee examined the *in vivo* use of BioGlue and its cytotoxic effects over cultured cells and various tissues. In this study, both human embryo fibroblasts and mouse myoblasts were used along with cells from

rabbit heart, lung and liver tissues. In the rabbit tissue studies, fibrin was used as a control. The authors found that the glutaraldehyde released from the BioGlue negatively affected the viability of cultured cells. In addition, when BioGlue was applied to rabbit lung and liver tissues, a severe inflammatory response was seen along with tissue necrosis. The authors note that these effects are less severe in the approved applications because the aorta is largely ECM components with lower cellular populations. The authors of this study concluded that the use of glutaraldehyde based adhesives should be limited to the current aortic applications because of the deleterious effects seen in other tissues [20]. St. Clair et al has also noted the cytotoxicity of aldehyde based adhesives, namely glutaraldehyde in their studies [21].

In addition to glutaraldehyde, a number of researchers have developed novel bioadhesives that utilize aldehyde groups for bond with tissues. Murakami et al developed a polymeric micelle composed of poly (ethylene glycol) and poly (DL-lactide) (PEG-PLA) terminated with aldehyde groups. The polymer in this study was known to be non-cytotoxic, while the crosslinker used had poor tissue permeability theoretically decrease possibly cytotoxic effects. The adhesive was evaluated for its hemostatic capabilities *in vivo* and was able to successfully stop bleeding in a variety of different applications. This novel adhesive performed similarly as a hemostatic agent when compared to the commercially available Tisseel, a fibrin based bioadhesive [138].

In addition to artificial polymeric materials for bioadhesion, natural materials have also been modified to form novel bioadhesives. Artzi et al developed an adhesive polymer made from PEG and dextran, a naturally occurring polysaccharide. In this study, the dextran was functionalized with aldehyde groups, which could be tailored to the

specific degree of adhesion required. The biocompatibility of the system was tested with rats *in vivo* and the researchers determined that there was inflammatory response from the adhesive that increased as the number of aldehyde groups on the functionalized dextran increased [12]. Shazly et al developed a hydrogel system that was a combination of both star PEG and a dextran aldehyde adhesive. The dextran aldehyde was synthesized through an oxidation reaction and reacted with tissues via the Schiff's base reaction. The adhesion of the polymer was tested on intestinal puncture wounds *in vitro* on its ability to resist bursting when pressure was increased, and performed successfully. The researchers noted that although increased aldehyde content can increase adhesion, steric interactions between adjacent aldehyde groups limit the adhesive ability. Additionally, the researchers noted that as the aldehyde content was increased, more interactions with amines took place decreasing the time for the polymer to form a consistent gel [13]. Bhatia et al also examined cytotoxic effects of a PEG amine and dextran aldehyde polymer adhesive in comparison with cyanoacrylate adhesive. In this study, mouse fibroblasts were placed in direct contact with the adhesive, which was found to be non-cytotoxic to cells, while cyanoacrylate adhesive was toxic to the same cells. Additionally, this dextran aldehyde adhesive did not cause an inflammatory response when placed in contact with mouse peritoneal macrophages [14].

Several researchers have also investigated chondroitin sulfate, a naturally occurring polysaccharide similar to dextran, as a novel bioadhesive. Reyes et al developed a chondroitin sulfate adhesive for sealing corneal incisions and tested *ex vivo*. The chondroitin sulfate was functionalized with aldehyde groups via an oxidation reaction and the adhesive was used to seal incisions to the cornea in comparison to

incisions sealed with sutures. When the pressure of the incision was examined, the adhesive sealed incisions were able to withstand twice to four times the amount of pressure as incisions sealed with sutures. Although the adhesive performed better than incisions sealed with sutures, the biocompatibility of this adhesive was not examined by the authors [15]. Wang et al also developed a chondroitin sulfate based adhesive, functionalized with both aldehyde and methacrylate groups, contained within a poly (ethylene glycol) diacrylate (PEGDA) hydrogel matrix. *In vitro* testing was performed on chondrocytes in direct contact with the chondroitin sulfate adhesive, which was applied using a brush. Chondrocytes were viable when examined over a five-week period in direct contact with the aldehyde-based adhesive, and incorporation of the hydrogel allowed the system to completely fill defects and increased ECM production by embedded cells [16]. Although aldehyde based adhesive systems are novel, additional researchers must investigate and address biocompatibility problems before future tissue engineering applications can be examined.

2.6 – Summary of Work

There is a need for a novel bioadhesive polymer scaffold that can support cell viability and encourage proliferation and differentiation not only *in vitro*, but also ultimately *in vivo*. This work investigates the development of a novel bioadhesive polymer that will be used to tissue engineer IVD tissue, specifically the NP. The polymer is comprised of several novel components, allowing it to create the ideal scaffold for repair and regeneration of damaged IVD tissues. This bioadhesive scaffold must maintain the biocompatibility of commonly used fibrin adhesives, however this scaffold needs to be stronger than the fibrin adhesive. Researchers have yet to develop a novel

bioadhesive scaffold, capable of supporting cell life, for tissue engineering applications relating to the IVD.

The proposed solution will include a polymer scaffold created of PNIPAAm grafted with CS. The PNIPAAm will be utilized for its thermosensitive properties, allowing the final scaffold to be implanted minimally invasively and to solidify *in situ*. Grafting chondroitin sulfate onto the polymer backbone will allow the system to have increased biocompatibility, decreased inflammatory response in the body, imbibe water, nutrients, enzymatic degradation characteristics and aid in cell proliferation and differentiation [18] [19]. Aldehyde functionalized chondroitin sulfate will serve as the adhesive component of this system. In this case, the chondroitin sulfate will be modified through an oxidation reaction, similar to that performed in Reyes et al, and will react with amines on the tissue surface via a Schiff's base reaction [15].

The ultimate goal of the scaffold and adhesive is to not only repair, but also regenerate IVD tissue. Therefore, cells must be encapsulated into the system and the cytotoxic effects of the aldehyde groups on the adhesive must be combatted. Lipid vesicles, or liposomes, are small particles composed of a lipid bilayer that can encapsulate a variety of materials. Liposomes have been used widely in many applications, specifically drug delivery applications, and therefore should be able to deliver ECM derivatives in our adhesive scaffold [139] [140] [141] [142]. Additionally, the lipids can be chosen in such a way that they melt at body temperature, in order to release the components within after adhesion has take place, but before cytotoxic events can occur [142]. Gelatin, a widely available and low cost protein, will be loaded into each

of the vesicles and has the ability to react with any remaining aldehyde groups via a Schiff's base reaction, preventing the cytotoxicity of the cells.

The final system will combine a PNIPAAm-CS copolymer, CS aldehyde, gelatin loaded lipid vesicles and cells for a novel tissue engineering strategy to repair the NP of the IVD. In this study, the adhesive strength, rheological properties, lower critical solution temperature behavior, and biocompatibility were examined and quantified.

Chapter 3

Materials and Methods

3.1 – Materials Synthesis and Characterization

3.1.1 – Poly (N-isopropylacrylamide) graft Chondroitin Sulfate Synthesis

Poly (N-isopropylacrylamide) graft chondroitin sulfate (PNIPAAm-g-CS) was synthesized in a 1000:1 molar ratio by reacting N-isoproylacrylamide (NIPAAm) monomer with chondroitin sulfate (CS) functionalized with methacrylate groups (mCS) through a procedure previously developed at Rowan University [143]. Chondroitin sulfate was functionalized using methacrylic anhydride (MAA) following a procedure adapted from Bryant et al [144]. A 25:1 molar ratio of methacrylic anhydride to CS was used resulting in a substitution of 0.1 methacrylate groups per repeat unit of CS, verified previously using H^1 nuclear magnetic resonance (NMR).

Methacrylated chondroitin sulfate was synthesized by dissolving 2 grams of CS (Sigma Aldrich) in 8 mL of de-ionized (DI) water. Once dissolved, the pH of the reaction mixture was corrected to 10 using 50% w/v sodium hydroxide (NaOH). When at the correct pH, 0.298 mL of MAA was added, and the mixture reacted while shaking for 24 hours at 60°C. The reaction can be seen in Figure 9. The mCS was then precipitated in 300-400 mL of cold acetone, vacuum filtered, and dried overnight in a vacuum oven prior to use.

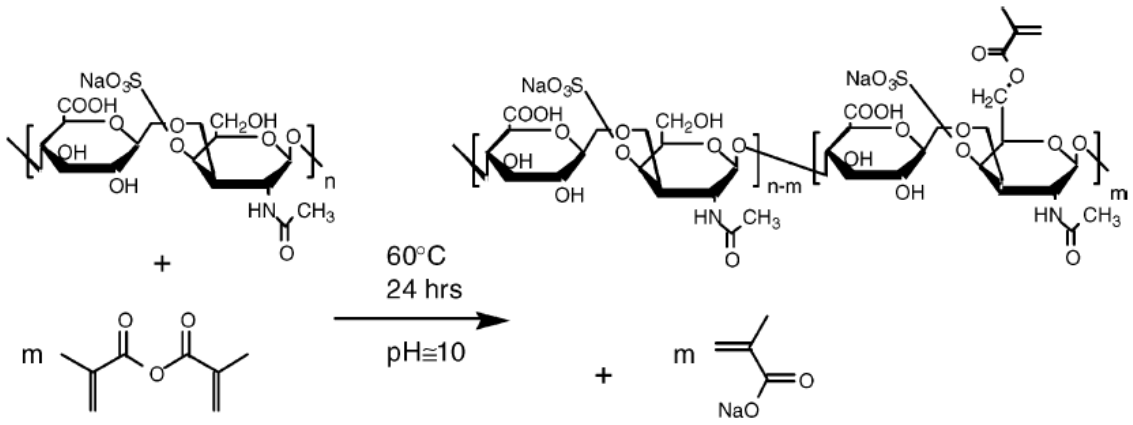

Figure 9: The reaction scheme for synthesizing mCS from CS and MAA [144]

NIPAAm (Acros) was first purified by dissolving in an excess amount of n-hexane at 60°C while stirring periodically, then recrystallized in an explosion proof freezer overnight. The recrystallized mixture was vacuum filtered and placed in the vacuum oven overnight to remove excess n-hexane. Purified NIPAAm was stored in the freezer prior to use.

PNIPAAm-g-CS was synthesized via redox polymerization by first dissolving 10 grams of NIPAAm and 2.209 g of mCS in 190 mL of DI water. The mixture was bubbled with nitrogen gas for a minimum of 15 minutes to remove excess oxygen. Once oxygen was removed, 0.8 mL of Tetramethylethylenediamine (TEMED) was added first, then 0.08 g of ammonium persulfate (APS) and the mixture was stirred vigorously for 15 seconds. The reaction was carried out for 24 hours under fluorescent lighting before placing the mixture into a 37°C incubator to aggregate. The PNIPAAm-g-CS was allowed to dialyze at 37°C for one week, with the PBS changed daily prior to lyophilization. Once dry, the polymer was hydrated as a 5% (w/v) solution in phosphate buffered saline (PBS) for use.

3.1.2 - Chondroitin Sulfate Aldehyde Synthesis

Chondroitin sulfate was oxidized in the presence of sodium periodate using a procedure similar to that presented in Reyes et al [15]. The oxidation allowed for the formation of aldehyde groups on the CS backbone creating a novel bioadhesive, as seen in Figure 10. Two grams of CS was dissolved in 40 mL of DI water and the mixture was bubbled with nitrogen gas for a minimum of 5 minutes. Two grams of sodium periodate were added and the reaction was carried out at room temperature in the dark while stirring for six hours. To stop the reaction, 0.55 mL of ethylene glycol was added to the reaction mixture and the mixture was allowed to stir for an additional hour [145]. The mixture was then placed into 3500 molecular weight cut off (MWCO) dialysis bags and dialyzed in DI water for a minimum of 24 hours. After the initial dialysis, the CS aldehyde was placed into a acetate buffer bath (pH 4.0, Fisher) for 3 hours before returning the CS aldehyde to dialysis in DI water for an additional 24 hours [146]. After dialysis, oxidized chondroitin sulfate was lyophilized for one week and stored in the fridge prior to use.

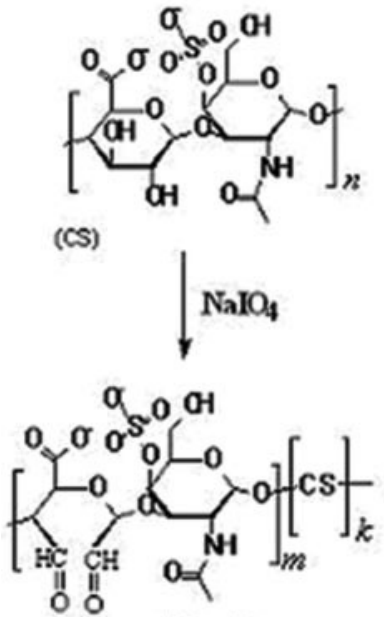

Figure 10: The reaction of CS with sodium periodate for form the bioadhesive CS aldehyde [15]

3.1.3 – Degree of CS aldehyde Substitution Determination

The degree of substitution (percentage of potential hydroxyl side groups converted to aldehyde groups) was measured through hydroxylamine hydrochloride titration using a procedure and calculations adapted from Zhao et al [147]. A solution of hydroxylamine hydrochloride (HH) was prepared by dissolving 17.5 g of HH in 130 mL of DI water. Additionally, 6 mL of methyl orange indicator was added and the solution was brought to a volume of 1L.

For each titration, 25 mL of HH solution was adjusted to a pH of 4 using 0.1N sodium hydroxide (Fisher) and 100 mg of CS aldehyde was subsequently dissolved into the HH solution. The mixture was titrated with 0.1N sodium hydroxide, recording

volume added and pH at 0.05 mL increments until the pH of the solution reached approximately 4.4.

The calculations to determine the degree of substitution for the CS aldehyde can be seen below as Equation 2-4. The change in pH was determined for each change in volume of sodium hydroxide added. The calculation of aldehyde substitution requires knowledge of the peak pH change per change in volume of titrant added (the derivative of the pH versus volume added plot) and can be seen graphically as Figure 11. In Equation 2, the total number of available hydroxyl groups was determined from the molecular weights of both the CS polymer and CS repeat unit. Subsequently in Equation 3 the number of aldehyde groups created through the oxidation reaction was calculated and this number was used in Equation 4 to calculate the percentage of aldehyde groups created through the oxidation of CS. It is important to note that in Equation 4 the numerator is divided by two because of the two hydroxyl groups present on each CS repeat unit.

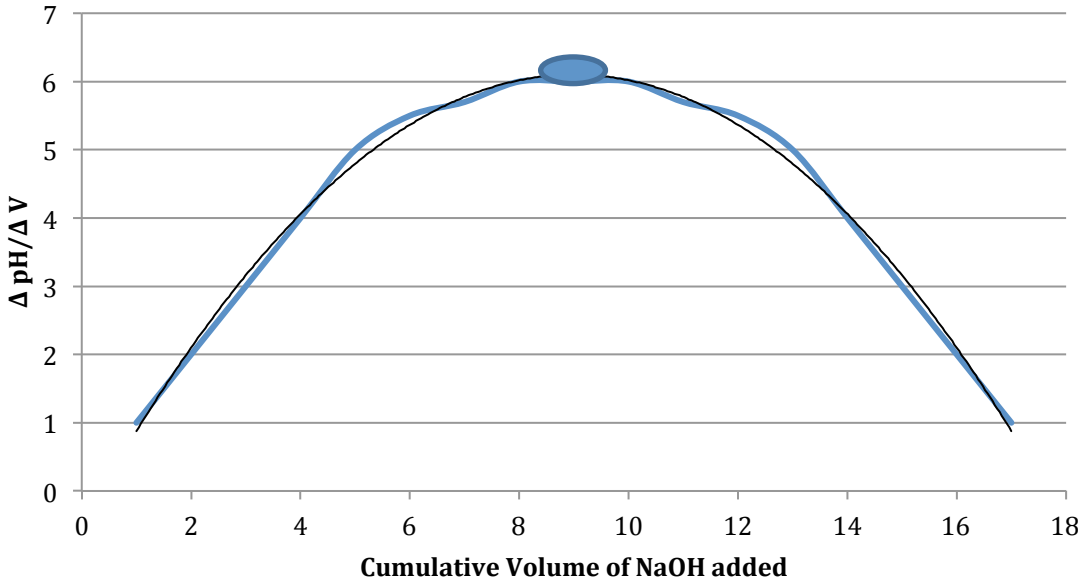

Figure 11: A graphical representation of the peak pH change per volume added to determine the cumulative volume of sodium hydroxide added

Equation 2: Calculation of the number of repeat units on each of the CS polymer chains (the MW of CS was 75,000, obtained from Sigma-Aldrich in August 2011)

$$\text{Number of Repeat Units} = \frac{\text{MW of CS Polymer}}{\text{MW of CS Repeat Unit}}$$

Equation 3: Calculation of moles of aldehyde groups present on the CS backbone (where V is the cumulative volume of sodium hydroxide added in liters at the largest pH change)

$$\frac{\text{Mole of Aldehyde Groups}}{\text{Mole of CS aldehyde}} = \frac{(\text{V})\ (\text{Molarity of NaOH})}{\text{Mole of CS Titrated}}$$

Equation 4: Calculation of the degree of substitution based on the number of available hydroxyl groups converted to aldehyde groups

$$\%\text{Conversion to Aldehyde} = \frac{\left({}^{Mole\ of\ Aldehyde\ Groups}/_{Mole\ of\ CS\ aldehyde}\right)/_{2}}{\text{Number of Repeat Units}}$$

3.1.4 – LCST Determination

The LCST was measured using the TA instruments Q2000 Differential Scanning Calorimeter (DSC). For each test between 5-15 mg of 5% (w/v) PNIPAAm-g-CS was placed into hermetically sealed aluminum dishes (pre-weighed) and the temperature was increased from 0-50°C at a rate of 10°C/min. LCST was determined by the endothermic peak on the DSC thermogram and the LCST was taken as the minimum of this peak.

3.1.5 – Rheological Characterization

Polymer viscosity was tested for each batch to ensure continuity in adhesion testing procedures. For each batch of 1000:1 PNP-CS polymer synthesized, 80 mL of a 5% solution was made by dissolving 4 grams of PNP-CS in 80 mL of PBS. Viscosity was tested using a using a Brookfield DV-11+ Viscometer with a #3 spindle and speed between 20-100 RPM. Average viscosity values were reported by averaging the viscosity measurements from 20-100 RPM and used to characterize each batch of PNIPAAm-g-CS.

3.1.6 – Mechanical Property Characterization

The mechanical properties of the adhesive were tested in tension based on the ASTM procedure 2258 for tissue adhesives in tension [148]. For testing and data collection, a Shimpo FGV-0.5X force gauge and Shimpo FGS-200PV E-Force Test Stand were used. Porcine ear cartilage, obtained from a local butcher, was cut into 1 cm^2

squares. One piece of cartilage was affixed a lower stainless steel weight and one piece of cartilage to the upper Teflon force gauge attachment. A sample of 0.1 mL was placed on the lower cartilage using a positive displacement pipette and the system was lowered applying 0.01 N of preload. Once preloaded, a solution of 0.9% sodium chloride heated to 37°C was added to completely cover the sample and mimic physiological conditions. The sodium chloride solution was maintained at 37°C throughout the entire test using a heating plate. The sample was allowed to form a hydrogel for five minutes prior to testing.

To test the material, force data was collected using the Shimpo E-Stand software. The material was separated at a rate of 2 mm/min until the adhesive had been separated or the test reached 7mm. A representative adhesion test can be seen in Figure 12. Stresses were calculated by subtracting the force exerted by the polymer from the buoyant force of a "blank" (Teflon attachment with cartilage alone raised at the same rate) and dividing by the cross sectional area of cartilage, as seen in Equation 5. The maximum stress was simply the highest stress obtained during the experiment, graphically the peak of the stress versus distance curve, seen below in Figure 13.

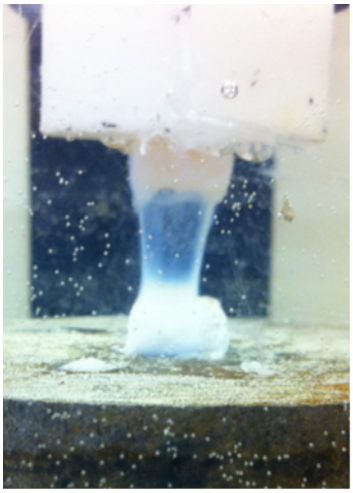

Figure 12: A representative adhesion test with adhesive between porcine cartilages

Equation 5: Calculation of stress by subtracting polymer force from the "blank" buoyant force and dividing by adhesive area

$$Stress = \frac{Force\ of\ Polymer - Buoyant\ Force}{Area\ of\ Cartilage}$$

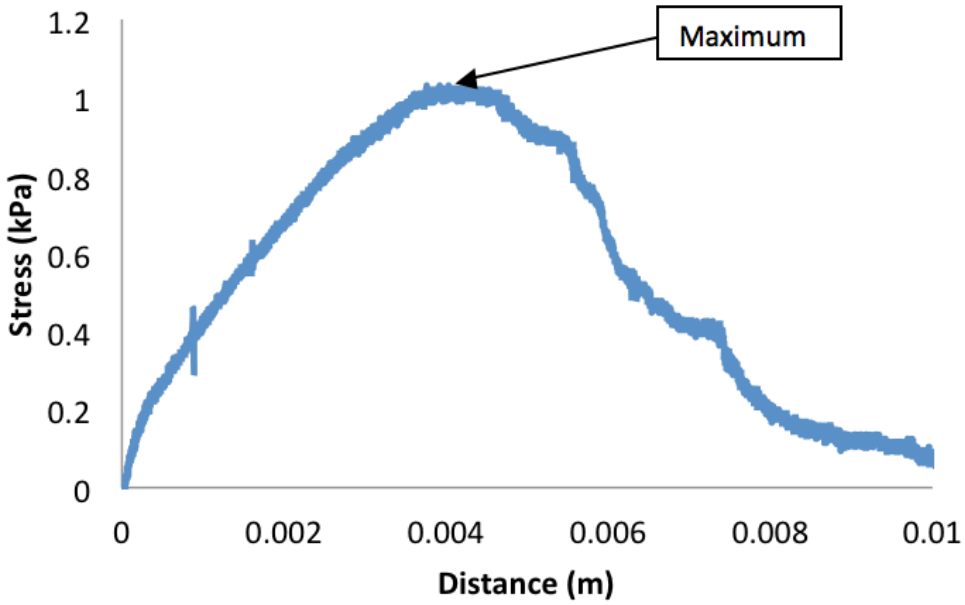

Figure 13: The graph of a representative adhesion test showing the maximum stress

3.1.7 – Liposome Synthesis and Release Studies

Liposomes have been widely used in experimentation as possible drug delivery vehicles. In this experimentation, liposomes were synthesized using well established "thin-film" methods [149] [150]. The lipids 1,2-dimyristoyl-sn-glycero-3-phosphocholine (DMPC) (Avanti Polar Lipids) (6.777 mg) and 1,2-dipalmitoyl-glycero-3-phosphocholine (DPPC) (Avanti Polar Lipids) (66.06 mg) were dissolved in 3.28 mL of chloroform and allowed to evaporate under vacuum overnight. The molar ratio of 90% DPPC and 10% DMPC was used to ensure the liposomes had a melting temperature of 37°C [151]. Dried lipids films were hydrated in a solution of gelatin in PBS at a concentration of 4 mg gelatin per mL and allowed to hydrate overnight at 60°C with vortexing periodically. Liposomes were then extruded with 11 passes through a 0.2 micron filter to break up

multilamellar vesicles. Once extruded, liposomes underwent dialysis at 4°C in 50,000 MWCO dialysis bags (Spectra/Por) for one week to remove un-entrapped gelatin. Finished liposomes were stored at 4°C prior to use.

Release studies were performed to quantify the amount of gelatin released. Loaded liposomes (1.5 mL) were placed into 50,000 MWCO dialysis bags and sealed in a glass jar containing 100 mL of DI water. The jar was stored at 37°C for 7 days and samples were taken from the water surrounding the dialysis bag. A standard solution of 0.02 mg/mL of gelatin was prepared in PBS and diluted according to Table 3.

Table 3: Preparation of known concentration solutions for the BCA assay

	Gelatin Solution (mL)	DI Water (mL)	Concentration (mg/mL)
1	6	0	0.02
2	5	1	0.01667
3	4	2	0.01333
4	3.5	2.5	0.01167
5	3	3	0.01
6	2.5	3.5	0.00833
7	2	4	0.00667
8	1.5	4.5	0.005
9	1	5	0.00333
10	0.5	5.5	0.00167
11	0	6	0

A bicinchoninic acid (BCA) assay (Micro BCA™ Protein Assay Kit – Pierce, Thermo Scientific) was used to quantify the amount of gelatin released from the loaded liposomes. The BCA working reagent was prepared according to the manufacturer instructions. The plate allowed to react for approximately two hours at 37°C before being

read at 562 nm using a Bio-Tek ELx800 plate reader. The standard curve was plotted in Excel and used as the correlation for determining the concentration released from the liposome samples.

3.2 – Biological Assays for Cell Viability

3.2.1 – Preparing Cells and Seeding Polymer Mixtures

To test the viability of cells within the polymer matrix, human embryonic kidney (HEK) 293 cells were utilized. Cell media was prepared by combining 90 mL Dulbecco's Modified Eagle Medium (Gibco) containing 4 mM L-Glutamine, 25 mM D-Glucose and 0.0399 mM Phenol Red with 5 mL Fetal Bovine Serum (FBS) (Gibco), 5 mL Calf Serum (Gibco) and 100 µL penicillin/streptomycin (Pen/Strep). HEK 293 cells were grown at 37°C until 85% confluent. Plates showing 85% confluence were subjected to treatment with 1 mL of trypsin and incubated at 37°C for 10 minutes to detach cells from the dish. After trypsinization, 5 mL of warm cell media was added to each plate and plates were combined into conical tube and lightly mixed to disperse cells.

Cell counts were performed with a hemocytometer counting in the specified pattern as stated in the instructions. Approximately 10 µL of cell mixture was loaded into the hemocytometer for counting. Two cell counts were performed for a given cell mix and averaged for calculations to obtain the average cell count C_A. To obtain a concentration of 10^6 cells per mL of polymer, Equation 6 and Equation 7 were used.

Equation 6: Using the average cell count from the hemocytometer, the initial concentration of cells within the mix was determined

$$(C_A)(6)(5)(10^4) = C_i = \frac{cells}{mL}$$

Equation 7: Calculation of the amount of cell mix needed to seed the polymer with 10^6 cells per mL (y is the volume of polymer being seeded, x is the volume of cell mixture required)

$$\frac{1\ mL\ C_i}{\frac{\left(\frac{C_i}{10^6}\right)}{3.3} - 1} = \frac{x\ mL\ C_i}{y\ - x}$$

The appropriate volume of cell mixture (x above) was combined with the proper volume of cell media (y-x above) and centrifuged at 1500 RPM at 4°C for 5 minutes to pellet cells. Once pelleted, the supernatant was removed and replaced with the proper amount of polymer mixture (y above). To ensure the cells were evenly distributed within the polymer, pipetting up and down approximately 20 times dispersed the pellet. Cell only controls were not subjected to centrifugation, simply diluted with the appropriate amount of cell media. For each of the assays, 300 µL of each polymer mix was added to the appropriate wells on a 24 well plate in triplicate. Polymer was allowed to aggregate at 37°C for 10 minutes prior to starting each assay and extruded water was removed. Cells were covered with cell media and incubated at 37°C for the desired time period prior to each assay. Prior to each assay, plates were removed from incubation and left at room

temperature for 24 hours to more easily separate seeded cells from the polymer formulations.

3.2.2 – PicoGreen Assay

The PicoGreen Assay (Invitrogen) was performed to quantitatively determine the amount of viable cells within the polymer by staining and counting the number of nucleotides present in each polymer and control solution mixture. To prepare the PicoGreen assay, a buffer solution of 1X TE (10 mM Tris-HCl, 1 mM EDTA, pH 7.5) was prepared by combining 5 mL of 10X TE solution and 45 mL of DNAse free water. Additionally, a "high range" solution of 2 µg/mL DNA was prepared by mixing 24 µl of the 0.5 µg/µL lamda DNA with 5.976 mL of TE buffer. This solution was diluted 40-fold to form the "low range" (50 ng/mL DNA) solution by mixing 150 µl of the 2 µg/mL DNA in 5.85 mL of TE buffer. Finally, the Quant-iT™ PicoGreen® reagent was prepared in the dark by first making a 200-fold dilution of DMSO in TE and combining this with a 150 µl Quant-iT™ PicoGreen® dsDNA reagent in 29.85 mL TE buffer. High and low range standard curves were prepared by combining TE Buffer, High or Low range DNA solutions and PicoGreen reagent according to Table 4 and Table 5.

Table 4: High range standard curve for the PicoGreen assay

Volume (µL) of TE	Volume (µL) of 2 µg/mL DNA Stock	Volume (µL) of Diluted Quant-iT™ PicoGreen® Reagent	Final DNA Concentration in Quant-iT™ PicoGreen® Assay
0	1,000	1,000	1 µg/mL
900	100	1,000	100 ng/mL
990	10	1,000	10 ng/mL
999	1	1,000	1 ng/mL
1,000	0	1,000	Blank

Table 5: Low range standard curve for the PicoGreen assay

Volume (µL) of TE	Volume (µL) of 50 ng/mL DNA Stock	Volume (µL) of Diluted Quant-iT™ PicoGreen® Reagent	Final DNA Concentration in Quant-iT™ PicoGreen® Assay
0	1,000	1,000	25 ng/mL
900	100	1,000	2.5 ng/mL
990	10	1,000	250 pg/mL
999	1	1,000	25 pg/mL
1,000	0	1,000	Blank

Polymer plates were incubated at 37°C for five days then allowed to gel at room temperature for 24 hours. Cells were first lysed with and DNA was extracted using the DNeasy Blood and Tissue kit (Qiagen) and following the manufacturer instructions. Approximately 1 mL of the PicoGreen reagent (150µL of PicoGreen in 29.85 mL of TE buffer) was added to each well of the 24 well plate and allowed to incubate at room temperature for 2-5 minutes protected from light. After incubation, 300 µL from each well was added to the well of a black 96-well plate and read in a spectrofluorometer or fluorescence at wavelengths of 480 nm for excitation and 520 nm for emission. Fluorescence values from a reagent blank were subtracted from each of the samples and

the corrected fluorescent readings for each of the standard curves was plotted to create a DNA concentration versus fluorescence correlation. This correlation was used to calculate the DNA concentration in each of the sample wells.

Chapter 4

Results and Discussion

Aim 1: Synthesize an adhesive copolymer consisting of poly (N-isopropylacrylamide) graft chondroitin sulfate blended with aldehyde modified chondroitin sulfate and characterize the material properties

The graft copolymer was synthesized in a molar ratio of 1000:1 (NIPAAm:mCS) and the lower critical solution behavior was verified through differential scanning calorimetry (DSC). The lower critical solution temperature of the copolymer was found to be between 30.5-31.5°C, slightly higher than the LCST of the homopolyer at 29.6°C, however still in the range to for a hydrogel *in situ*. The increase in LCST was also seen by other researchers and can be attributed to an increase in water content of the copolymer, requiring more energy to break the additional hydrogen bonds formed with the PNIPAAm below the LCST [152] [153]. Additionally, rheology was used as an indicator of molecular weight range. It was determined that using consistent viscosity will yield consistent adhesion testing results. The rheological characteristics of solutions containing 5% (w/v) PNIPAAm-g-CS were examined and found to have optimal adhesive characteristics when the average viscosity ranged from 800-1000 cP.

Chondroitin sulfate aldehyde (CS aldehyde) was synthesized using various mass ratios of sodium periodate to chondroitin sulfate. Mass ratios of 0.5:1, 1:1 and 2:1 of sodium periodate:CS were used to generate varying degrees of substitution, converting a different number of hydroxyl groups present on the CS backbone to aldehyde groups. The aldehyde degree of substitution was tested using the hydroxylamine hydrochloride titration method adapted from Zhao et al [147]. These different ratios yielded degrees of

substitution seen below in Table 6. Each of the mass ratios used produced a statistically different ($p<0.05$) degree of substitution on the CS aldehyde.

Table 6: The effect of varying the mass ratio of sodium periodate to CS on degree of substitution

Mass Ratio Sodium Periodate : CS	0.5:1	1:1	2:1
Average Degree of Substitution (%)	33.86	42.39	72.17
95% Confidence Interval (%)	1.24	3.06	14.45

Tensile testing using a solution of 5% (w/v) PNIPAAm-g-CS hydrated in phosphate buffered saline (PBS) combined with 3% (w/v) CS aldehyde using the three degrees of substitution was carried out. As seen in Figure 14, varying the degree of substitution of CS aldehyde produces no statistically significant ($p>0.05$) differences in the adhesive strength of the copolymer. However, using the 5% PNIPAAm-g-CS solution as a control, it can be seen that the incorporation of any degree of substitution CS aldehyde produces a statistically significant ($p<0.05$) increase in adhesive strength over samples containing no CS aldehyde. It is theorized that while more aldehyde groups may be present with increased CS aldehyde degree of substitution, the reaction is limited by how many of these aldehyde groups can reach the surface, therefore causing no increase in adhesion with more aldehyde groups present.

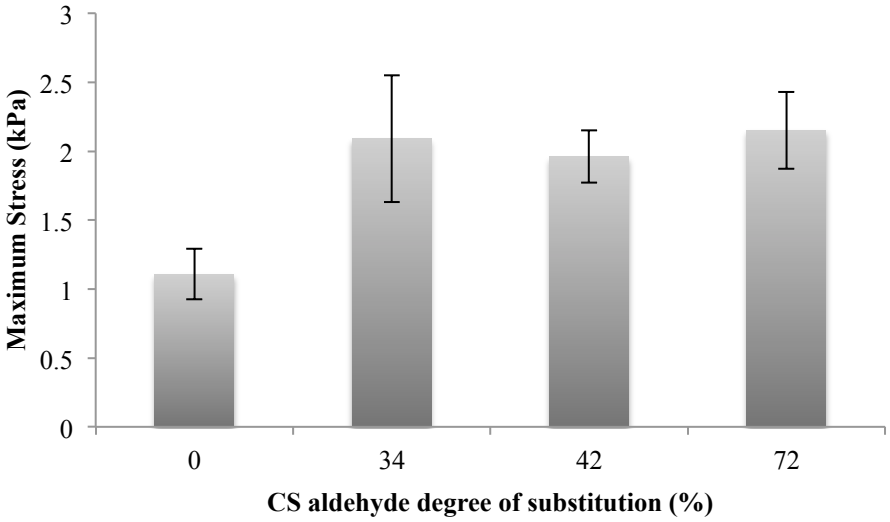

Figure 14: The effects of varying degree of substitution on maximum stress (error bars represent 95% confidence intervals)

Although the results show limited variability in the adhesive strength of the scaffold, it is important to recall the biocompatibility of the system can be affected by the presence of excess aldehyde groups as shown in literature [20] [21]. Therefore there is no benefit to increasing the degree of substitution of CS aldehyde. Optimization of the system should, therefore, only focus on minimizing the cytotoxic effects of CS aldehyde on surrounding cells and tissues. For this reason, it is important to choose a lower degree of substitution that has minimal effects on cell life. In subsequent testing, a degree of substitution of 42% CS aldehyde was used.

Next, the effects of varying the concentration of CS aldehyde within the polymer matrix were investigated. The degree of substitution for these tests was held constant at 42% while the concentrations of CS aldehyde concentrations in copolymer solution at

room temperature were varied from 0, 1, 3 and 5% (w/v). Tensile tests results for varied weight percentage of CS aldehyde can be seen in Figure 15.

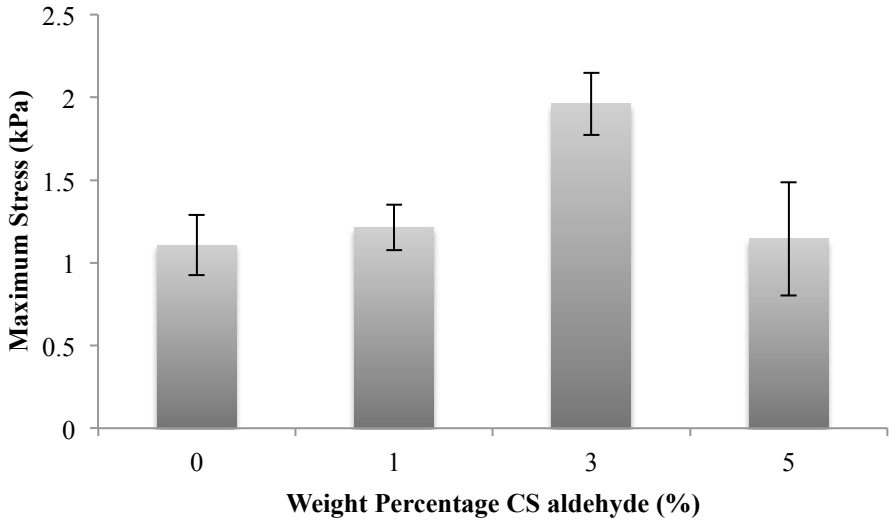

Figure 15: The effects of varying weight percentage of CS aldehyde in copolymer solution at room temperature on maximum stress (error bars represent 95% confidence intervals)

In these tests, 3% CS aldehyde was shown to have a statistically ($p<0.05$) higher maximum stress. The concentration of CS aldehyde within shows an increase in adhesive strength from no CS aldehyde to 3% CS aldehyde where there is a maximum. This indicates that increasing CS aldehyde concentration initially increases the adhesive strength. Above 3% CS aldehyde, the adhesive strength begins to decrease. Formulations of 5% CS aldehyde showed an increase in viscosity that can be attributed to the decrease in adhesive strength beyond 3% CS aldehyde. To achieve maximum adhesion, mechanical interlocking must take place between the uneven surface of the tissue and the

CS aldehyde adhesive filling these voids and forming the covalent bonds via the Schiff's base reaction. With an increased viscosity sample, it is more difficult for the polymer to fill these voids on the tissue surface and therefore the adhesive strength of the sample decreases as the viscosity of the sample increases.

In summary, in Aim 1 it was determined that the copolymer had a LCST of between 30.5-31.5°C, an increase over the homopolymer which had an LCST of approximately 29.6°C. Additionally, the copolymer performed optimally in adhesive testing when the viscosity ranged from 800-1000 cP. There were found to be no increases in the adhesive strength of the polymer when the degree of substitution was increase, likely limited by the number of available reaction sites on the cartilage and aldehyde groups able to reach these reaction sites. Finally, varying weight percentage showed that the highest adhesive strength was achieved using a solution containing 3% (w/v) CS aldehyde, above this critical concentration, the viscosity increases too drastically and adhesive strength decreases.

Aim 2: Prepare lipid vesicles hydrated with ECM derivatives, verify ECM derivative release, and combine lipid vesicles with the scaffold prepared in Aim 1 and characterize the adhesive properties of the system.

To combat the cytotoxic effects of aldehyde groups, ECM loaded lipid vesicles (liposomes) were used as a controlled release mechanism, assuming that excess aldehyde groups would react with the ECM derivative upon liposome melting at body temperature. Theoretically, heating of the polymer allows the Schiff's base reaction with the tissue to take place, ensuring maximum adhesion, prior to the release of gelatin from the liposomes. However, liposome melting should be fast enough to prevent cytotoxic events

from occurring after adhesion with the CS aldehyde and tissue has occurred. Gelatin was chosen as the ECM derivative because of its low cost. Lipid vesicles (22.2 mg dry lipids per mL of solution) hydrated in a solution of 4 mg/mL of gelatin in PBS were shown to release approximately 0.622 mg gelatin/mL of solution, verified with a BCA assay after seven days of release at 37°C. Negligible amounts of gelatin were released at 4°C.

Tensile testing was used to determine the effects of liposome concentration on adhesion. Samples containing 5% (w/v) PNIPAAm-g-CS and 3% (w/v) CS aldehyde were used. Liposomes hydrated with 4 mg/mL of gelatin were diluted to obtain solutions with 0, 2.78, 5.55, 11.1 and 22.2 mg dry lipids per mL of liposome solution. The results of tensile testing results can be in Figure 16.

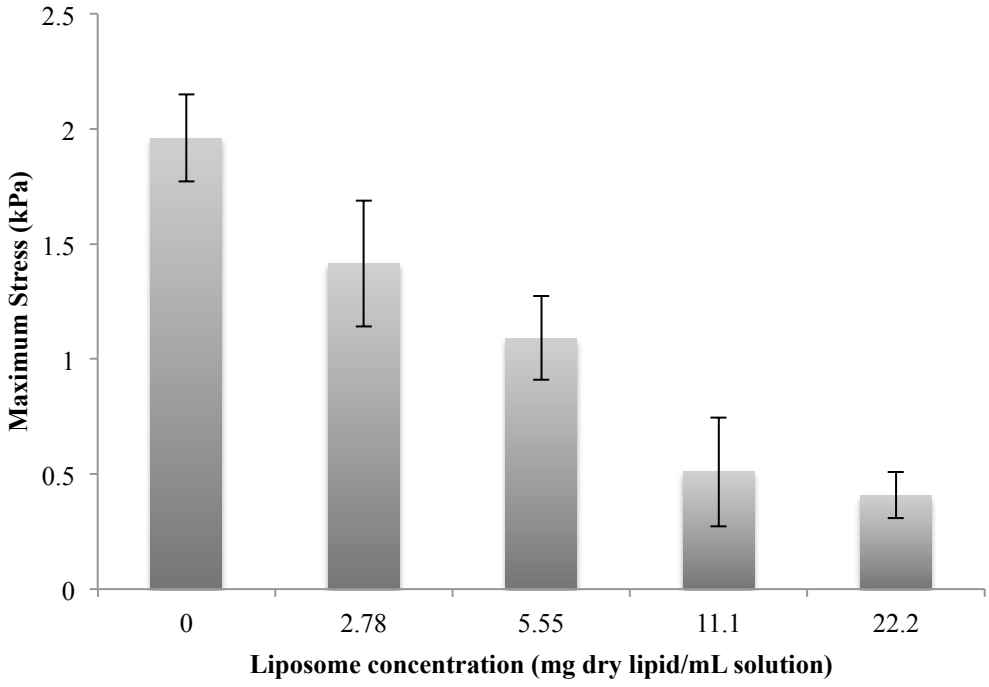

Figure 16: The effects of varying liposome concentration in room temperature copolymer solution on maximum stress (error bars represent 95% confidence intervals)

It can be seen that increasing the liposome concentration causes a significant decrease in the adhesive strength of the copolymer solution, however this could be attributed to either the lipid or gelatin component of the liposomes. It was theorized that the lipid component was preventing mechanical interlocking, and therefore effect adhesion from taking place and this was investigated further.

In order to determine the effect of each component, tensile tests were performed using samples containing no lipids (free gelatin) and samples with no gelatin (unloaded liposomes) in comparison with the adhesive properties of systems with copolymer only, copolymer and adhesive and copolymer adhesive and liposome samples. All solutions contained 5% (w/v) PNIPAAm-g-CS and solutions with adhesive contained 3% (w/v) CS aldehyde. The CS aldehyde degree of substitution was again held constant at 42%. Tensile test results for adhesive strength can be seen in Figure 17.

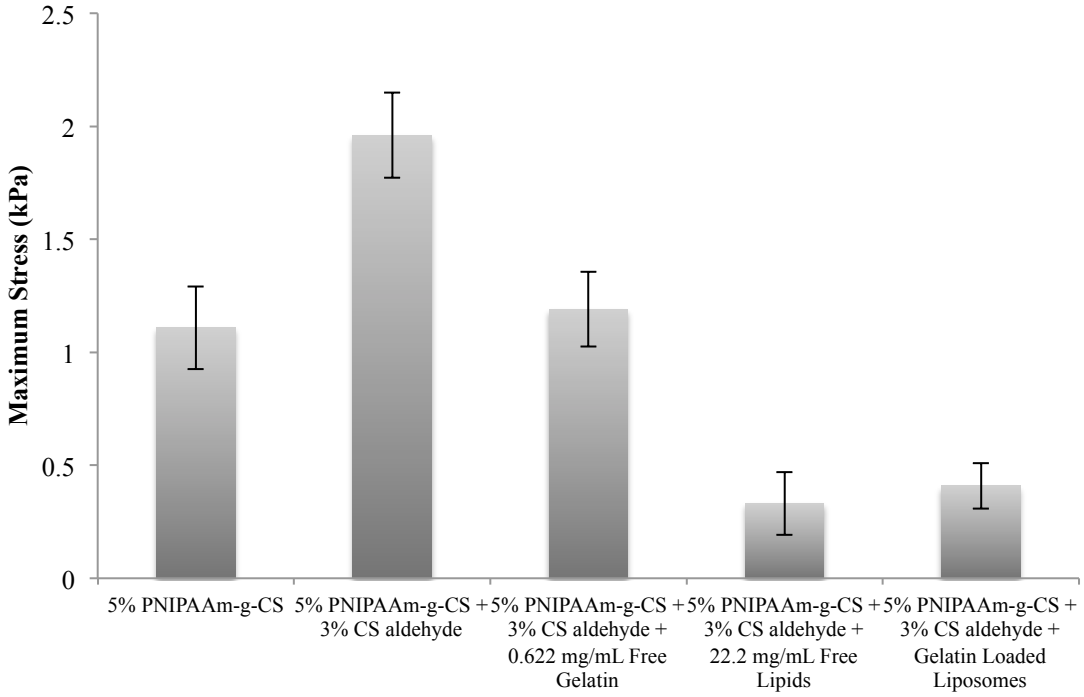

Figure 17: The effects of lipids, gelatin and liposomes on maximum stress (error bars represent 95% confidence intervals)

The addition of free gelatin at a concentration comparable to what was measured in the liposome release studies slightly reduced adhesive strength to a level that was statistically similar to that seen with PNIPAAm-g-CS alone, indicating the need for encapsulation of gelatin. The addition of both lipids, loaded or unloaded, significantly ($p<0.05$) decreased maximum stress. The decrease in adhesive strength from liposome addition (loaded and unloaded) to the matrix is thought to have occurred by interacting the interface of adhesive and tissue. As was previously mentioned, the adhesive component of the system relies on mechanical interlocking to take place in order to form effective covalent bonds with the tissues. The liposomes, being composed of fatty acids,

are thought form a "slippery layer" which prohibits the CS aldehyde from effectively contacting the tissue surface and therefore covalent and hydrogen bonds cannot form.

Incorporation of increasing amounts of CS aldehyde causes an increase in the adhesive strength of the polymer matrix, while incorporation of increasing lipid content causes a decrease in adhesive strength, a result expected from the study with free gelatin, loaded and unloaded liposomes.

Aim 3: Demonstrate the ability of the tissue engineering scaffold to support encapsulated cell survival

The biocompatibility of the polymer system was examined using the solution that presented the highest adhesive properties (5% PNIPAAm-g-CS with 3% CS aldehyde) and the solution that would release the maximum amount of gelatin (5% PNIPAAm-g-CS with 3% CS aldehyde and 22.2 mg dry lipids/mL). It was hypothesized that solutions with no liposomes should show signs of cytotoxicity from aldehyde groups present on the CS aldehyde adhesive, while solutions containing liposomes would show a recovery in the biocompatibility of the system. Human embryonic kidney (HEK) 293 cells were used to examine the biocompatibility and were seeded within the aforementioned adhesive scaffolds at a density of 10^6 cells per mL for 5 days at 37°C. Additionally, the biocompatibility of the polymer alone was examined. As a control, a monolayer of cells without polymer was used. A PicoGreen assay was used to examine the biocompatibility and results can be seen in Figure 18.

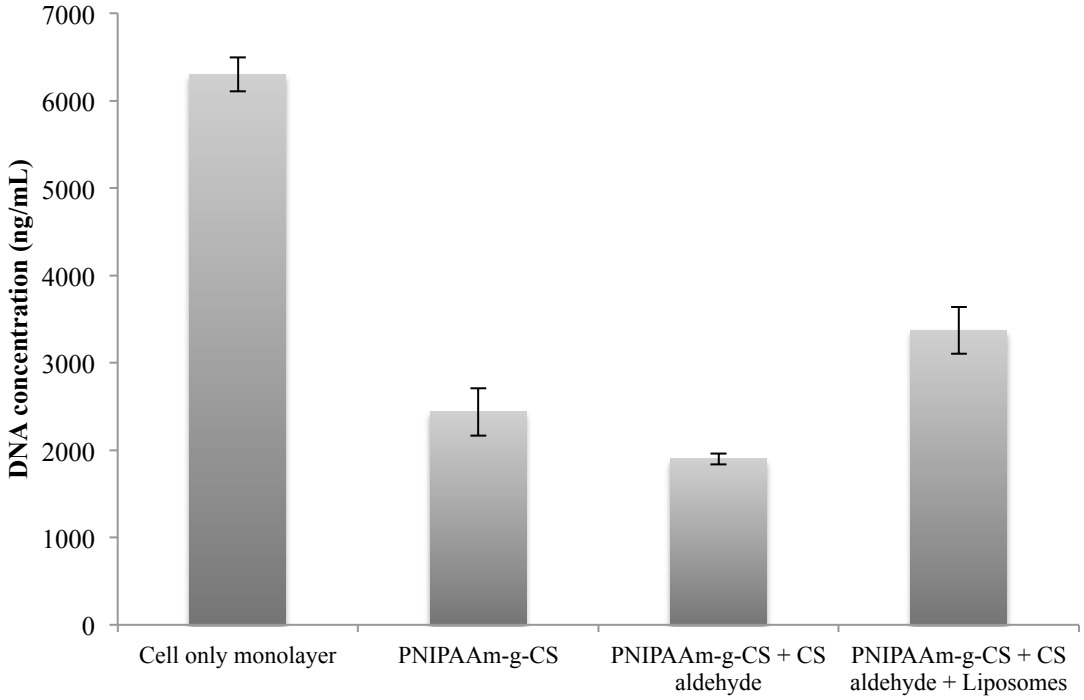

Figure 18: Biocompatibility of polymer formulations with and without liposomes, compared with polymer only and cell only control samples. Cells were seeded at 10^6 cells per mL and incubated for 5 days at 37°C (error bars represent standard deviation)

The biocompatibility of the system performed as expected. The addition of CS aldehyde into the system causes a decrease in the biocompatibility, likely due to the presence of excess aldehyde groups. Addition of liposomes allows for the release of gelatin and an increase in the overall biocompatibility of the system. Additionally, it appears that the liposomes were able to release gelatin quickly enough to prevent cytotoxic events from occurring, a criteria for their use in the adhesive scaffold. While these results seem to indicate a biocompatible system, additional preliminary biocompatibility testing (data and procedures shown in Appendix A) seems to indicate that liposomes may contribute to the cytotoxicity of the system.

Overall, there are conflicting choices when optimizing both the biocompatibility and maximum adhesion of the system. These data demonstrate that the optimum adhesive system is one containing no lipid component, as the lipids negatively affect the adhesive strength. Conversely, the optimal biocompatible system is one that contains some way of incorporating an ECM derivative to interact with the excess aldehyde groups present from the adhesive CS aldehyde. As an alternative of achieving the release of gelatin into the system, gelatin loaded alginate microparticles could be examined. Alginate makes an appealing choice because, as a polysaccharide like CS, alginate could theoretically hydrogen bond with the tissue surface, theoretically having adhesive characteristics of the graft copolymer alone. In this system, alginate would be crosslinked and physically entrap the gelatin within, allowing for the release based on diffusion principles. Additionally, alternative methods for increasing the adhesion could be examined, including adhesives that may present more favorable biocompatibility characteristics while increasing the overall adhesive strength of the system. In addition, to optimize the system a number of other characteristics can be examined. These include looking at the degradation of the system, MSC differentiation *in vitro*, and the compressive mechanical characteristics over time. In future work, these avenues should be examined as a means of creating a tissue engineered scaffold with optimal characteristics for both adhesion and cell survival *in vitro*.

Chapter 5

Conclusions and Recommendations

In this work a novel, *in situ* forming, adhesive hydrogel scaffold was synthesized and characterized. A copolymer scaffold of PNIPAAm-g-CS was synthesized and the LCST was found to be between 30.5-31.5°C, a slight increase over the homopolymer with a LCST of 29.6°C. In addition, CS aldehyde was also successfully synthesized and the degree of substitution was verified through hydroxylamine hydrochloride titration. The adhesive CS aldehyde was successfully synthesized with three degrees of substitution by varying the mass ratio of sodium periodate, the oxidizing agent, in the reaction. These degrees of substitution are specifically, 33, 42 and 72%.

The mechanical properties of the copolymer and adhesive were examined. First, the degree of substitution of CS aldehyde was tested with a copolymer only control. The degree of substitution was found to have no impact on the adhesive strength of the scaffold, however incorporation of CS aldehyde produced significantly higher ($p<0.05$) adhesive strength than the copolymer alone. From this, it was concluded that for maximum biocompatibility, the system with fewer aldehyde groups should be used for subsequent testing. For this reason, all subsequent testing used a CS aldehyde degree of substitution of 42%. Additionally, the weight percentage of CS aldehyde within the copolymer scaffold was varied. The adhesive properties of adhesive scaffold containing 0, 1, 3 and 5% (w/v) CS aldehyde were tested. Initially, incorporation of more CS aldehyde increased the adhesive strength, up to the optimum of 3% (w/v) CS aldehyde. This was an expected result, as more aldehyde groups present should form more bonds with the tissue surface. When the weight percentage of CS aldehyde was increased to 5%

(w/v), there was a marked increase in the viscosity of the sample, observed during experimentation. It is theorized that this viscosity increased prevented samples of 5% (w/v) CS aldehyde from mechanically interlocking with the tissue and therefore causing a decrease in the adhesive properties of the system at this concentration.

In an effort to increase the biocompatibility of the system, ECM loaded lipid vesicles were synthesized. Liposomes were formulated to melt at body temperature and hydrated in solutions of 4 mg/mL gelatin in PBS. These liposomes were shown to release approximately 0.622 mg gelatin/mg dry lipids over a 7 day period at 37°C. Additionally, the mechanical properties of the adhesive system were examined with lipid vesicles incorporated throughout. The concentration of lipids was varied in a system containing 5% (w/v) PNIPAAm-g-CS in PBS and 3% (w/v) CS aldehyde. This system showed as lipid concentration increased, there was a decreasing trend in the adhesive strength of the system. In an effort to determine if this was the effect of the gelatin released from the liposomes or the lipids themselves, the mechanical properties of each component of the liposomes was examined. When un-encapsulated gelatin ("free gelatin") was included in the system, the adhesive strength was statistically similar to the grafter copolymer alone, indicating the need for encapsulation. Additionally, including both loaded and unloaded lipid vesicles caused a significant decrease ($p<0.05$) in adhesive strength over both copolymer alone and copolymer with CS aldehyde. This decrease in adhesive strength could be attributed to the lipid component of the liposomes. This is theorized to be a result of lipids preventing mechanical interlocking from taking place at the tissue surface by forming a "slippery layer" at the interface of the scaffold and tissue.

Finally, the preliminary biocompatibility of the adhesive scaffold was examined by encapsulating HEK 293 cells. Formulations containing 5% (w/v) PNIPAAm-g-CS, 5% (w/v) PNIPAAm-g-CS with 3% (w/v) CS aldehyde and 5% (w/v) PNIPAAm-g-CS with 3% (w/v) CS aldehyde and 22.2 mg/mL liposomes were seeded with HEK 293 cells at a density of 10^6 cells/mL and incubated at 37 for 5 days. These preliminary results demonstrate that the grafted copolymer alone is relatively biocompatible when compared to the cell only control. Addition of CS aldehyde adhesive into the system causes a decrease in the biocompatibility, likely due to the presence of excess aldehyde groups, while incorporation of liposomes causes a recovery in the biocompatibility of the scaffold, likely due to the release of gelatin in the system. Ultimately, these results indicate that the thermally triggered release of gelatin from lipid vesicles is sufficient to cause an increase in biocompatibility.

While it was demonstrated that there is a need for gelatin encapsulation and that liposomes are capable of encapsulating and releasing gelatin to maintain the biocompatibility of the system, lipids were shown to significantly ($p<0.05$) decrease the adhesive strength of the system. Therefore, future work should investigate the use of alternative encapsulation methods for the controlled release of gelatin within the adhesive scaffold. One technology that could be of particular interest is the release of gelatin using alginate microparticles. These alginate particles could be synthesized simply using a solution of sodium alginate and calcium as the divalent crosslinking agent. In current research, this method has been shown capable to encapsulating and releasing growth factor via simple diffusion [154]. Additionally, because alginate is a polysaccharide

component, much like CS, it is theorized that adhesive strength should be at least similar to the grafted copolymer alone.

In addition to examining the encapsulation of gelatin, examining the adhesive properties of the system further should be considered in future work. Specifically, the adhesive strength of CS aldehyde should be compared to commercially available adhesives, such as fibrin. Fibrin should be subjected to the same test protocol as the CS aldehyde adhesive examined in this work, allowing for comparable data. By comparing CS aldehyde to fibrin, the determination can be made as to if there is a sufficient increase in the adhesive strength by incorporating CS aldehyde or if alternative adhesive chemistry needs to be examined.

Overall, the adhesive system developed shows promise for the repair and regeneration of damaged IVD tissue. The optimal adhesive properties were shown to occur with a weight percentage of 3% (w/v) CS aldehyde, and encapsulation of gelatin with lipid vesicles was shown to increase the biocompatibility of the system over systems with no lipid vesicles. While alternative encapsulation techniques have the potential to increase the biocompatibility of the system while maintaining adhesive properties, this work has made large strides in the development of adhesive scaffolds for IVD repair.

List of References

[1] X. Lou, R. Pietrobon, S. X Sun, G. G. Liu, and L. Hey, "Estimates and Patterns of Direct Health Care Expenditures Among Individuals With Back Pain in the United States," *Spine*, vol. 29, no. 1, pp. 79–86, 2004.

[2] R. A. Deyo and Y.-J. Tsui-Wu, "Descriptive Epidemiology of Low-back Pain and Its Related Medical Care in the United States," *Spine*, vol. 12, no. 3, pp. 264–268, 1987.

[3] L. Shvartzman, E. Weingarten, H. Sherry, S. Levin, and A. Persaud, "Cost-Effectiveness Analysis of Extended Conservative Therapy Versus Surgical Intervention in the Management of Herniated Lumbar Intervertebral Disc," *Spine*, vol. 17, no. 2, pp. 176–182, 1992.

[4] M. V. Risbud, T. J. Albert, A. Guttapalli, E. J. Vresilovic, A. S. Hillibrand, A. R. Vaccaro, and I. M. Shapiro, "Differentiation of Mesenchymal Stem Cells Towards a Nucleus Pulposus-like Phenotype In Vitro: Implications for Cell-Based Transplantation Therapy," *Spine*, vol. 29, no. 23, pp. 2627–2632, 2009.

[5] V. Duance, J. Crean, T. Sims, N. Avery, S. Smith, J. Menage, S. Eisenstein, and R. S, "Changes in collagen cross-linking in degenerative disc disease and scoliosis," *Spine*, vol. 23, no. 23, pp. 2545–2451, 1998.

[6] H. Pokhama and F. Phillips, "Collagen crosslinks in human lumbar intervertebral disc aging," *Spine*, vol. 23, no. 15, pp. 1645–1648, 1998.

[7] E. Cassinelli and J. Kang, "Current understanding of lumbar disc degeneration," *Operative Techniques in Orthopaedics*, vol. 10, no. 4, pp. 254–262, 2000.

[8] H. Beuff, Ulrich and W. Van Der Reis, "Low Back Pain," *Orthopedics*, vol. 23, no. 2, pp. 345–364, 1996.

[9] R. Lanza, R. Langer, and J. Vacanti, Eds., *Principles of Tissue Engineering*, 3rd ed. Academic Press, 2007.

[10] B. R. Whatley and X. Wen, “Intervertebral disc (IVD): Structure, degeneration, repair and regeneration,” *Materials Science and Engineering: C*, vol. 32, no. 2, pp. 61–77, Mar. 2012.

[11] H. Wilke, F. Heuer, C. Neidlinger-Wilke, and L. Claes, “Is a collagen scaffold for a tissue engineered nucleus replacement capable of restoring disc height and stability in an animal model?,” *European Spine Journal*, vol. 15, no. SUPPL. 3, pp. S433–S438, 2006.

[12] N. Artzi, T. Shazly, A. B. Baker, A. Bon, and E. R. Edelman, “Aldehyde-amine chemistry enables modulated biosealants with tissue-specific adhesion.,” *Advanced materials (Deerfield Beach, Fla.)*, vol. 21, no. 32–33, pp. 3399–403, Sep. 2009.

[13] T. M. Shazly, N. Artzi, F. Boehning, and E. R. Edelman, “Viscoelastic adhesive mechanics of aldehyde-mediated soft tissue sealants.,” *Biomaterials*, vol. 29, no. 35, pp. 4584–91, Dec. 2008.

[14] S. K. Bhatia, S. D. Arthur, H. K. Chenault, and G. K. Kodokian, “Interactions of polysaccharide-based tissue adhesives with clinically relevant fibroblast and macrophage cell lines.,” *Biotechnology letters*, vol. 29, no. 11, pp. 1645–9, Nov. 2007.

[15] J. M. G. Reyes, S. Herretes, A. Pirouzmanesh, D.-A. Wang, J. H. Elisseeff, A. Jun, P. J. McDonnell, R. S. Chuck, and A. Behrens, “A modified chondroitin sulfate aldehyde adhesive for sealing corneal incisions.,” *Investigative ophthalmology & visual science*, vol. 46, no. 4, pp. 1247–50, Apr. 2005.

[16] D.-A. Wang, S. Varghese, B. Sharma, I. Strehin, S. Fermanian, J. Gorham, D. H. Fairbrother, B. Cascio, and J. H. Elisseeff, “Multifunctional chondroitin sulphate for cartilage tissue-biomaterial integration.,” *Nature materials*, vol. 6, no. 5, pp. 385–92, May 2007.

[17] S. Fujishige, K. Kubota, and I. Ando, “Phase Transition of Aqueous Solutions of Poly(N-isopropylacrylamide) and Poly(N-isopropylmethacrylamide),” *Journal of Physical Chemistry*, vol. 93, no. 8, pp. 3311–3313, 1989.

[18] I. Strehin, Z. Nahas, K. Arora, T. Nguyen, and J. Elisseeff, “A versatile pH sensitive chondroitin sulfate-PEG tissue adhesive and hydrogel.,” *Biomaterials*, vol. 31, no. 10, pp. 2788–97, May 2010.

[19] S. Varghese, N. S. Hwang, A. C. Canver, P. Theprungsirikul, D. W. Lin, and J. Elisseeff, "Chondroitin sulfate based niches for chondrogenic differentiation of mesenchymal stem cells.," *Matrix biology : journal of the International Society for Matrix Biology*, vol. 27, no. 1, pp. 12–21, Jan. 2008.

[20] W. Fürst and A. Banerjee, "Release of glutaraldehyde from an albumin-glutaraldehyde tissue adhesive causes significant in vitro and in vivo toxicity.," *The Annals of thoracic surgery*, vol. 79, no. 5, pp. 1522–8; discussion 1529, May 2005.

[21] M. St. Clair, E. Bermudez, E. Gross, B. Butterworth, L. Recio, and A. Carrano, "Evaluation of the genotoxic potential of glutaraldehyde," *Environmental and Molecular Mutagenesis*, vol. 18, no. 2, pp. 113–119, 1991.

[22] G. W. Jenkins, C. P. Kemnitz, and G. J. Tortora, *Anatomy and Physiology from Science to Life*, 1st ed. Wiley, 2007, pp. 221–230.

[23] S. Grad, M. Alini, D. Eglin, D. Sakai, J. Mochida, S. Mahor, E. Collin, B. Dash, and A. Pandit, "Cells and biomaterials for intervertebral disc regeneration," *Synthesis Lectures on Tissue Engineering*, vol. 5, no. 1, pp. 1–104, 2010.

[24] F. Marchand and A. M. Ahmed, "Investigation of the laminate structure of lumbar disc anulus fibrosus," *Spine*, vol. 15, no. 5, pp. 402–410, 1990.

[25] A. Maroudas, R. A. Stockwell, A. Nachemson, and J. Urban, "Factors involved in the nutrition of the human lumbar intervertebral disc: cellularity and diffusion of glucose in vitro.," *Journal of anatomy*, vol. 120, no. Pt 1, pp. 113–30, Sep. 1975.

[26] N. L. Nerurkar, D. M. Elliott, and R. L. Mauck, "Mechanical design criteria for intervertebral disc tissue engineering.," *Journal of biomechanics*, vol. 43, no. 6, pp. 1017–30, Apr. 2010.

[27] J. I. Sive, P. Baird, M. Jeziorsk, a Watkins, J. a Hoyland, and a J. Freemont, "Expression of chondrocyte markers by cells of normal and degenerate intervertebral discs.," *Molecular pathology : MP*, vol. 55, no. 2, pp. 91–7, Apr. 2002.

[28] J. Clouet, G. Grimandi, M. Pot-Vaucel, M. Masson, H. B. Fellah, L. Guigand, Y. Cherel, E. Bord, F. Rannou, P. Weiss, J. Guicheux, and C. Vinatier, "Identification of phenotypic discriminating markers for intervertebral disc cells and articular chondrocytes.," *Rheumatology (Oxford, England)*, vol. 48, no. 11, pp. 1447–50, Nov. 2009.

[29] N. Bogduk, *Clinical anatomy of the lumbar spine and sacrum*, 4th ed. Elsevier Health Sciences, 2005.

[30] Q. B. Bao, G. M. McCullen, P. a Higham, J. H. Dumbleton, and H. a Yuan, "The artificial disc: theory, design and materials.," *Biomaterials*, vol. 17, no. 12, pp. 1157–67, Jun. 1996.

[31] W. Johannessen and D. M. Elliott, "Effects of degeneration on the biphasic material properties of human nucleus pulposus in confined compression," *Spine*, vol. 30, no. 24, pp. E724–729, 2005.

[32] B. A. Best, F. Guilak, L. A. Setton, W. Zhu, F. Saed-Nejad, A. Ratcliffe, M. Weidenbaum, and V. C. Mow, "Compressive mechanical properties of the human anulus fibrosus and their relationship to biochemical composition.," *Spine*, vol. 19, no. 2, p. 212, 1994.

[33] J. C. Iatridis, L. a Setton, R. J. Foster, B. a Rawlins, M. Weidenbaum, and V. C. Mow, "Degeneration affects the anisotropic and nonlinear behaviors of human anulus fibrosus in compression.," *Journal of biomechanics*, vol. 31, no. 6, pp. 535–44, Jun. 1998.

[34] D. Périé, D. Korda, and J. C. Iatridis, "Confined compression experiments on bovine nucleus pulposus and annulus fibrosus: sensitivity of the experiment in the determination of compressive modulus and hydraulic permeability.," *Journal of biomechanics*, vol. 38, no. 11, pp. 2164–71, Nov. 2005.

[35] H. L. Guerin and D. M. Elliott, "Quantifying the contributions of structure to annulus fibrosus mechanical function using a nonlinear, anisotropic, hyperelastic model," *Journal of Orthopaedic Research*, vol. 25, no. 4, pp. 508–516, 2007.

[36] M. Kasra, M. Parnianpour, a Shirazi-Adl, J. L. Wang, and M. D. Grynpas, "Effect of strain rate on tensile properties of sheep disc anulus fibrosus.," *Technology and health care : official journal of the European Society for Engineering and Medicine*, vol. 12, no. 4, pp. 333–42, Jan. 2004.

[37] L. A. Setton and D. M. Elliott, “Anisotropic and inhomogeneous tensile behavior of the human anulus fibrosus: experimental measurement and material model predictions,” *Journal of biomechanical engineering*, vol. 123, no. 3, pp. 256–263, 2001.

[38] H. A. L. Guerin and D. M. Elliott, “Degeneration affects the fiber reorientation of human annulus fibrosus under tensile load.,” *Journal of biomechanics*, vol. 39, no. 8, pp. 1410–8, Jan. 2006.

[39] Y. Fujita, N. A. Duncan, and J. C. Lotz, “Radial tensile properties of the lumbar annulus fibrosus are site and degeneration dependent,” *Journal of Orthopaedic Research*, vol. 15, no. 6, pp. 814–819, 1997.

[40] S. Ebara, J. C. Iatridis, L. A. Setton, R. J. Foster, V. C. Mow, and M. Weidenbaum, “Tensile properties of nondegenerate human lumbar anulus fibrosus,” *Spine*, vol. 21, no. 4, pp. 452–461, 1996.

[41] E. R. Acaroglu, J. C. Iatridis, L. A. Setton, R. J. Foster, V. C. Mow, and M. Weidenbaum, “Degeneration and aging affect the tensile behavior of human lumbar anulus fibrosus,” *Spine*, vol. 20, no. 24, pp. 2690–2701, 1995.

[42] G. D. O’Connell, S. Sen, D. H. Cortes, and D. M. Elliott, “Biaxial mechanics are Inhomogeneous and Altered with Degeneration in the Human Annulus Fibrosus,” in *Transactions of the 56rd Annual Meeting of the Orthopaedic Research Society*, 2010.

[43] C. Wang, J. D. Auerbach, W. R. T. Witschey, R. a Balderston, R. Reddy, and A. Borthakur, “Advances in Magnetic Resonance Imaging for the assessment of degenerative disc disease of the lumbar spine.,” *Seminars in spine surgery*, vol. 19, no. 2, pp. 65–71, Jun. 2007.

[44] M. C. Battie, T. Videman, K. Gill, G. B. Moneta, R. Nyman, J. Kaprio, and M. Koskenvou, “Volvo Award in Clinical Sciences: Smoking and Lumbar Intervertebral Disc Degeneration: An MRI Study of Identical Twins,” *Spine*, vol. 16, no. 9, pp. 1015–1021, 1991.

[45] M. Pope, M. Magnusson, and D. Wilder, “Kappa Delta Award. Low back pain and whole body vibration,” *Clinical Orthopaedics and Related Research*, pp. 241–248, 1998.

[46] M. C. Battie, T. Videman, L. E. Gibbons, L. Fisher, H. Manninen, and K. Gill, "Determinants of Lumbar Disc Degeneration: A Study Relating Lifetime Exposures and Magnetic Resonance Imaging Findings in Identical Twins," *Spine*, vol. 20, no. 24, pp. 2601–2612, 1995.

[47] R. S. Lee, M. V Kayser, and S. Y. Ali, "Calcium phosphate microcrystal deposition in the human intervertebral disc.," *Journal of anatomy*, vol. 208, no. 1, pp. 13–9, Jan. 2006.

[48] G. Lyons, S. Eisenstein, and M. Sweet, "Biochemical changes in intervertebral disc degeneration," *Biochimica et Biophysica Acta (BBA) - General Subjects*, vol. 673, pp. 443–453, 1981.

[49] J. Urban and S. Roberts, "Degeneration of the intervertebral disc," *Arthritis Research and Therapy*, vol. 5, no. 3, pp. 120–130, 2003.

[50] J. Crean, S. Roberts, D. C. Jaffray, S. Eisenstein, and V. Duance, "Matrix metalloproteinases in the human intervertebral disc: role in disc degeneration and scoliosis," *Spine*, vol. 22, no. 24, pp. 2877–2884, 1997.

[51] M. a Adams, D. S. McNally, and P. Dolan, "'Stress' distributions inside intervertebral discs. The effects of age and degeneration.," *The Journal of bone and joint surgery. British volume*, vol. 78, no. 6, pp. 965–72, Nov. 1996.

[52] R. J. Moore, B. Vernon-Roberts, R. D. Fraser, O. Osti, and M. Schembri, "The Origin and Fate of Herniated Lumbar Intervertebral Disc Tissue," *Spine*, vol. 21, no. 18, pp. 2149–2155, 1996.

[53] K. Fujita, T. Nakagawa, K. Hirabayashi, and Y. Nagai, "Neutral Proteinases in Human Intervertebral Disc: Role in Degeneration and Probable Origin," *Spine*, vol. 18, no. 13, pp. 1766–1773, 1993.

[54] I. Spiliopoulou, P. Korovessis, D. Konstantinou, and G. Dimitracopoulos, "IgG and IgM Concentration in the Prolapsed Human Intervertebral Disc and Sciatica Etiology," *Spine*, vol. 19, no. 12, pp. 1320–1323, 1994.

[55] S. S. Rajaee, H. W. Bae, L. E. a Kanim, and R. B. Delamarter, "Spinal fusion in the United States: analysis of trends from 1998 to 2008.," *Spine*, vol. 37, no. 1, pp. 67–76, Jan. 2012.

[56] H. H. Bohlman, S. E. Emery, D. B. Goodfellow, and P. K. Jones, "Robinson anterior cervical discectomy and arthrodesis for cervical radiculopathy. Long-term follow-up of one hundred and twenty-two patients," *The Journal of bone and joint surgery*, vol. 75, no. 9, pp. 1298–1307, 1993.

[57] M. A. Rousseau, D. S. Bradford, R. Bertagnoli, S. S. Hu, and J. C. Lotz, "Disc arthroplasty design influences intervertebral kinematics and facet forces.," *The spine journal*, vol. 6, no. 3, pp. 258–66, 2006.

[58] C. K. Lee, "Accelerated Degeneration of the Segment Adjacent to a Lumbar Fusion," *Spine*, vol. 13, no. 3, pp. 375–377, 1988.

[59] "DePuy Synthes," 2012. [Online]. Available: www.depuy.com. [Accessed: 05-Jul-2012].

[60] "DePuy Synthes," 2012. [Online]. Available: www.synthes.com. [Accessed: 05-Jul-2012].

[61] C. M. Bono and S. R. Garfin, "History and evolution of disc replacement.," *The Spine Journal*, vol. 4, p. 145S–150S, 2004.

[62] S. L. Griffith, A. P. Shelokov, K. Buttner-Janz, J. P. LeMarie, and W. S. Zeegers, "A multicenter retrospective study of the clinical results of the LINK® SB Charite intervertebral prosthesis: The initial European experience," *Spine*, vol. 19, no. 16, pp. 1842–1849, 1994.

[63] R. B. Delemarter, D. M. Fribourg, L. E. A. Kanim, and H. Bae, "ProDisc artificial total lumbar disc replacement: Introduction and early results from the United States clinical trial," *Spin*, vol. 28, no. 20, pp. S167–S175, 2003.

[64] G. Denozière and D. N. Ku, "Biomechanical comparison between fusion of two vertebrae and implantation of an artificial intervertebral disc.," *Journal of biomechanics*, vol. 39, no. 4, pp. 766–75, Jan. 2006.

[65] F. Geisler, S. Blumenthal, R. Guyer, P. McAfee, J. Regan, J. Johnson, and B. Mullin, "Neurological complications of lumbar artificial disc replacement and comparison of clinical results with those related to lumbar arthrodesis in the literature: results of a multicenter, prospective, randomized investigational device exemption study of Cha," *Journal of Neurosurgery: Spine*, vol. 1, no. 2, pp. 143–154, 2004.

[66] B. W. Cunningham, “Basic scientific considerations in total disc arthroplasty,” *The Spine Journal*, vol. 4, no. 6, pp. S219–S230, 2004.

[67] E. R. S. Ross, “Revision in artificial disc replacement.,” *The Spine Journal*, vol. 9, no. 9, pp. 773–5, Sep. 2009.

[68] A. Van Ooji, F. Cumhur Oner, and A. Verbout, “Complications of artificial disc replacement: A report of 27 patients with the SB charité disc,” *Journal of Spine Disorders and Techniques*, vol. 16, no. 4, pp. 369–383, 2003.

[69] J. Rawlinson, K. Punga, K. Gunsallus, D. Bartel, and T. Wright, “Wear simulation of the ProDisc-L disc replacement using adaptive finite element analysis,” *Journal of Neurosurgery: Spine*, vol. 7, no. 2, pp. 165–173, 2007.

[70] P. Klara and C. Ray, “Artificial nucleus replacement: Clinical experience,” *Spine*, vol. 27, no. 12, pp. 1374–1377, 2002.

[71] C. Ray, “The PDN® prosthetic disc-nucleus device,” *European Spine Journal*, vol. 11, no. Supplemental 2, pp. S137–S142, 2002.

[72] B. D. Ratner, A. S. Hoffman, F. J. Schoen, and J. E. Lemons, Eds., *Biomaterials Science: An Introduction to Materials in Medicine*. Academic Press, 2004.

[73] G. M. McCullen and H. A. Yuan, “Artificial disc: Current developments in artificial disc replacement,” *Current Opinion in Orthopaedics*, vol. 14, no. 3, pp. 138–143, 2003.

[74] C. Shim, S. Lee, C. Park, and W. Choi, “Partial disc replacement with the PDN prosthetic disc nucleus device: early clinical results,” *Journal of spinal*, vol. 16, no. 4, pp. 324–30, Aug. 2003.

[75] D. F. Williams, *The Williams Dictionary of Biomaterials*. Liverpool University Press, 1999.

[76] P. Revell, E. Damien, L. Di Silvio, N. Gurav, C. Longinotti, and L. Ambrosio, “Tissue engineered intervertebral disc repair in the pig using injectable polymers,” *Journal of Materials Science: Materials in Medicine*, vol. 18, no. 2, pp. 303–308, 2007.

[77] J. Cloyd, N. Malhorta, L. Weng, W. Chen, R. L. Mauck, and D. M. Elliott, "Material properties in unconfined compression of human nucleus pulposus, injectable hyaluronic acid-based hydrogels and tissue engineering scaffolds," *European Spine Journal*, vol. 16, no. 11, pp. 1892–1898, 2007.

[78] L. J. Nesti and W.-J. Li, "Intervertebral Disc Tissue Engineering Using a Novel Hyaluronic Acid–Nanofibrous Scaffold (HANFS) Amalgam," *Tissue Engineering - Part A*, vol. 14, no. 9, pp. 1527–1537, 2008.

[79] A. I. Chou, S. O. Akintoye, and S. B. Nicoll, "Photo-crosslinked alginate hydrogels support enhanced matrix accumulation by nucleus pulposus cells in vivo.," *Osteoarthritis and cartilage / OARS, Osteoarthritis Research Society*, vol. 17, no. 10, pp. 1377–84, Oct. 2009.

[80] H. Mizuno, A. K. Roy, C. A. Vacanti, K. Kojima, M. Ueda, and L. J. Bonassar, "Tissue-Engineered Composites of Anulus Fibrosus and Nucleus Pulposus for Intervertebral Disc Replacement," *Spine*, vol. 29, no. 12, pp. 1290–1297, 2004.

[81] E. Thonar, H. An, and K. Masuda, "Compartmentalization of the matrix formed by nucleus pulposus and annulus fibrosus cells in alginate gel," *Biochemical Society Transactions*, vol. 30, pp. 874–878, 2002.

[82] K. Chiba, G. B. J. Andersson, K. Masuda, S. Momohara, J. Williams, and E. Thonar, "A New Culture System to Study the Metabolism of the Intervertebral Disc In Vitro," *Spine*, vol. 23, no. 17, pp. 1821–1827, 1998.

[83] H. Gruber, E. Fisher, B. Desai, and A. Stasky, "Human intervertebral disc cells from the annulus: three-dimensional culture in agarose or alginate and responsiveness to TGF- β1," *Experimental cell*, vol. 235, no. 1, pp. 13–21, Aug. 1997.

[84] W. C. Hutton, W. a Elmer, L. M. Bryce, E. E. Kozlowska, S. D. Boden, and M. Kozlowski, "Do the intervertebral disc cells respond to different levels of hydrostatic pressure?," *Clinical biomechanics (Bristol, Avon)*, vol. 16, no. 9, pp. 728–34, Nov. 2001.

[85] M. Kasra, V. Goel, J. Martin, S.-T. Wang, W. Choi, and J. Buckwalter, "Effect of dynamic hydrostatic pressure on rabbit intervertebral disc cells.," *Journal of orthopaedic research : official publication of the Orthopaedic Research Society*, vol. 21, no. 4, pp. 597–603, Jul. 2003.

[86] D. Sakai and J. Morchida, “Stem cell applications in cell therapy for nucleus repair,” *European Cells and Materials*, vol. 10, no. Supplemental 3, p. 43, 2005.

[87] H. Gruber, J. Ingram, K. Leslie, H. Norton, and E. J. Hanley, “Cell shape and gene expression in human intervertebral disc cells: in vitro tissue engineering studies,” *Biotechnic & Histochemistry*, vol. 78, no. 2, pp. 109–117, 2003.

[88] C. Neidlinger-Wilke, K. Würtz, A. Liedert, C. Schmidt, W. Börm, A. Ignatius, H.-J. Wilke, and L. Claes, “A three-dimensional collagen matrix as a suitable culture system for the comparison of cyclic strain and hydrostatic pressure effects on intervertebral disc cells.,” *Journal of neurosurgery. Spine*, vol. 2, no. 4, pp. 457–65, Apr. 2005.

[89] M. Alini, W. Li, P. Markovic, M. Aebi, R. Spiro, and P. Roughley, “The potential and limitations of a cell-seeded collagen/hyaluronan scaffold to engineer an intervertebral disc-like matrix,” *Spine*, vol. 28, no. 5, pp. 446–454, 2003.

[90] D. O. Halloran, S. Grad, M. Stoddart, P. Dockery, M. Alini, and A. S. Pandit, “An injectable cross-linked scaffold for nucleus pulposus regeneration.,” *Biomaterials*, vol. 29, no. 4, pp. 438–47, Mar. 2008.

[91] P. Roughley, C. Hoemann, E. DesRosiers, F. Mwale, J. Antoniou, and M. Alini, “The potential of chitosan-based gels containing intervertebral disc cells for nucleus pulposus supplementation.,” *Biomaterials*, vol. 27, no. 3, pp. 388–96, Jan. 2006.

[92] F. Mwale, M. Iordanova, C. N. Demers, T. Steffen, P. Roughley, and J. Antoniou, “Biological Evaluation of Chitosan Salts Cross-Linked to Genipin as a Cell Scaffold for Disk Tissue Engineering,” *Tissue Engineering - Part A*, vol. 11, no. 1–2, pp. 130–140, 2005.

[93] C. Séguin, M. D. Grynpas, R. M. Pilliar, S. Waldman, and R. A. Kandel, “Tissue Engineered Nucleus Pulposus Tissue Formed on a Porous Calcium Polyphosphate Substrate,” *Spine*, vol. 29, no. 12, pp. 1299–1306, 2004.

[94] D. J. Hamilton, C. a Séguin, J. Wang, R. M. Pilliar, and R. a Kandel, “Formation of a nucleus pulposus-cartilage endplate construct in vitro.,” *Biomaterials*, vol. 27, no. 3, pp. 397–405, Jan. 2006.

[95] S.-H. Yang, P.-Q. Chen, Y.-F. Chen, and F.-H. Lin, “An in-vitro study on regeneration of human nucleus pulposus by using gelatin/chondroitin-6-sulfate/hyaluronan tri-copolymer scaffold.,” *Artificial organs*, vol. 29, no. 10, pp. 806–14, Oct. 2005.

[96] C. Li, B. Huang, G. Luo, C. Zhang, Y. Zhuang, and Y. Zhou, “Construction of collagen II/hyaluronate/chondroitin-6-sulfate tri-copolymer scaffold for nucleus pulposus tissue engineering and preliminary analysis of its physico-chemical properties and biocompatibility,” *Journal of Materials Science: Materials in Medicine*, vol. 21, no. 2, pp. 741–751, 2010.

[97] J. Thomas, K. Gomes, A. Lowman, and M. Marcolongo, “The Effect of Dehydration History on PVA/PVP Hydrogels for Nucleus Pulposus Replacement,” *Journal of biomedical materials research - Part B Applied Biomaterials*, vol. 69, no. 2, pp. 135–140, 2004.

[98] A. Joshi, G. Fussell, J. Thomas, A. Hsuan, A. Lowman, A. Karduna, E. Vresilovic, and M. Marcolongo, “Functional compressive mechanics of a PVA/PVP nucleus pulposus replacement.,” *Biomaterials*, vol. 27, no. 2, pp. 176–84, Jan. 2006.

[99] K. Saldanha, S. Piper, K. Ainsile, T. Desai, H. Kim, and S. Majumdar, “Magnetic resonance imaging of iron oxide labelled stem cells: Applications to tissue engineering based regeneration of the intervertebral disc,” *European Cells and Materials*, vol. 16, pp. 17–25, 2008.

[100] D. Ruan, H. Xin, C. Zhang, C. Wang, C. Xu, C. Li, and Q. He, “Experimental intervertebral disc regeneration with tissue-engineered composite in a canine model,” *Tissue Engineering - Part A*, vol. 16, no. 7, pp. 2381–2389, 2010.

[101] S. M. Richardson, J. M. Curran, R. Chen, A. Vaughan-Thomas, J. a Hunt, A. J. Freemont, and J. A. Hoyland, “The differentiation of bone marrow mesenchymal stem cells into chondrocyte-like cells on poly-L-lactic acid (PLLA) scaffolds.,” *Biomaterials*, vol. 27, no. 22, pp. 4069–78, Aug. 2006.

[102] J. Gan, P. Ducheyne, E. Vresilovic, and I. M. Shapiro, “Bioactive glass serves as a substrate for maintenance of phenotype of nucleus pulposus cells of the intervertebral disc,” *Journal of Biomedical Materials Research Part A*, vol. 51, no. 4, pp. 596–604, 2000.

[103] P. Freeman and J. Rowlinson, “Lower critical points in polymer solutions,” *Polymer*, vol. 1, pp. 20–26, 1960.

[104] Y. Akiyama, A. Kikuchi, M. Yamato, and T. Okano, "Ultrathin poly(N-isopropylacrylamide) grafted layer on polystyrene surfaces for cell adhesion/detachment control.," *Langmuir : the ACS journal of surfaces and colloids*, vol. 20, no. 13, pp. 5506–11, Jun. 2004.

[105] S. Kim and K. E. Healy, "Synthesis and characterization of injectable poly(N-isopropylacrylamide-co-acrylic acid) hydrogels with proteolytically degradable cross-links.," *Biomacromolecules*, vol. 4, no. 5, pp. 1214–23, 2003.

[106] S. Ohya, Y. Nakayama, and T. Matsuda, "Thermoresponsive artificial extracellular matrix for tissue engineering: hyaluronic acid bioconjugated with poly(N-isopropylacrylamide) grafts.," *Biomacromolecules*, vol. 2, no. 3, pp. 856–63, Jan. 2001.

[107] J.-P. Chen and T.-H. Cheng, "Thermo-responsive chitosan-graft-poly(N-isopropylacrylamide) injectable hydrogel for cultivation of chondrocytes and meniscus cells.," *Macromolecular bioscience*, vol. 6, no. 12, pp. 1026–39, Dec. 2006.

[108] R. Stile, W. Burghardt, and K. E. Healy, "Synthesis and characterization of injectable poly (N-isopropylacrylamide)-based hydrogels that support tissue formation in vitro," *Macromolecules*, vol. 32, pp. 7370–7379, 1999.

[109] N. Comolli, B. Neuhuber, I. Fischer, and A. Lowman, "In vitro analysis of PNIPAAm-PEG, a novel, injectable scaffold for spinal cord repair.," *Acta biomaterialia*, vol. 5, no. 4, pp. 1046–55, May 2009.

[110] L. Conova, J. Vernengo, Y. Jin, B. T. Himes, B. Neuhuber, I. Fischer, and A. Lowman, "A pilot study of poly(N-isopropylacrylamide)-g-polyethylene glycol and poly(N-isopropylacrylamide)-g-methylcellulose branched copolymers as injectable scaffolds for local delivery of neurotrophins and cellular transplants into the injured spinal cord.," *Journal of Neurosurgery: Spine*, vol. 15, no. 6, pp. 594–604, Dec. 2011.

[111] J. Vernengo, G. Fussell, and N. Smith, "Evaluation of novel injectable hydrogels for nucleus pulposus replacement," *Journal of Biomedical*, vol. 84B, no. 1, pp. 64–69, 2008.

[112] J. Vernengo, G. W. Fussell, N. G. Smith, and A. M. Lowman, "Synthesis and characterization of injectable bioadhesive hydrogels for nucleus pulposus replacement and repair of the damaged intervertebral disc.," *Journal of biomedical materials research. Part B, Applied biomaterials*, vol. 93, no. 2, pp. 309–17, May 2010.

[113] A. Trott, "Cyanoacrylate Tissue Adhesives," *JAMA: the journal of the American Medical Association*, pp. 2–3, 1997.

[114] B. Petersen, A. Barkun, S. Carpenter, P. Chotiprasidhi, R. Chuttani, W. Silverman, N. Hussain, J. Liu, G. Taitelbaum, and G. G. Ginsberg, "Tissue adhesives and fibrin glues.," *Gastrointestinal endoscopy*, vol. 60, no. 3, pp. 327–33, Sep. 2004.

[115] J. S. Pollak and R. I. White, "The Use of Cyanoacrylate Adhesives in Peripheral Embolization," *Journal of Vascular and Interventional Radiology*, pp. 907–913, 2001.

[116] A. J. Singer, J. V Quinn, and J. E. Hollander, "The cyanoacrylate topical skin adhesives.," *The American journal of emergency medicine*, vol. 26, no. 4, pp. 490–6, May 2008.

[117] D. M. Toriumi, W. F. Raslan, M. Friedman, and M. E. Tardy, "Histotoxicity of cyanoacrylate tissue adhesives. A comparative study.," *Archives of otolaryngology--head & neck surgery*, vol. 116, no. 5, pp. 546–50, May 1990.

[118] H. Vinters, K. Galil, M. Lundie, and J. Kaufman, "The histotoxicity of cyanoacrylates. A selective review," *Neuroradiology*, vol. 27, no. 4, pp. 279–291, 1985.

[119] A. Ekelund and O. S. Nilsson, "Tissue adhesives inhibit experimental new bone formation," *International orthopaedics*, pp. 331–334, 1991.

[120] L. J. Reckers, D. J. Fagundes, and M. Cohen, "The ineffectiveness of fibrin glue and cyanoacrylate on fixation of meniscus transplants in rabbits.," *The Knee*, vol. 16, no. 4, pp. 290–4, Aug. 2009.

[121] R. A. Chivers and R. G. Wolowacz, "The strength of adhesive-bonded tissue joints," *International Journal of Adhesion and Adhesives*, vol. 17, no. 2, pp. 127–132, May 1997.

[122] A. Sharma, R. Kaur, S. Kumar, P. Gupta, S. Pandav, B. Patnaik, and A. Gupta, "Fibrin glue versus N-butyl-2-cyanoacrylate in corneal perforations.," *Ophthalmology*, vol. 110, no. 2, pp. 291–8, Feb. 2003.

[123] B. Jamnadas-Khoda, M. a a Khan, G. P. L. Thomas, and S. J. Ghosh, "Histoacryl glue: a burning issue.," *Burns : journal of the International Society for Burn Injuries*, vol. 37, no. 1, pp. e1–3, Feb. 2011.

[124] F. J. Papatheofanis, "Cytotoxicity of alkyl-2-cyanoacrylate adhesives," *Journal of Biomedical Materials Research*, vol. 23, no. 6, pp. 661–668, 1989.

[125] "Baxter," 2012. [Online]. Available: www.baxter.com. [Accessed: 07-Aug-2012].

[126] M. Brittberg, E. Sjögren-Jansson, a Lindahl, and L. Peterson, "Influence of fibrin sealant (Tisseel) on osteochondral defect repair in the rabbit knee.," *Biomaterials*, vol. 18, no. 3, pp. 235–42, Feb. 1997.

[127] W. Bensaid, J. T. Triffitt, C. Blanchat, K. Oudina, L. Sedel, and H. Petite, "A biodegradable fibrin scaffold for mesenchymal stem cell transplantation," *Biomaterials*, vol. 24, no. 14, pp. 2497–2502, Jun. 2003.

[128] K. L. Christman, A. J. Vardanian, Q. Fang, R. E. Sievers, H. H. Fok, and R. J. Lee, "Injectable fibrin scaffold improves cell transplant survival, reduces infarct expansion, and induces neovasculature formation in ischemic myocardium.," *Journal of the American College of Cardiology*, vol. 44, no. 3, pp. 654–60, Aug. 2004.

[129] Y. Yamada, J. Seong Boo, R. Ozawa, T. Nagasaka, Y. Okazaki, K. Hata, and M. Ueda, "Bone regeneration following injection of mesenchymal stem cells and fibrin glue with a biodegradable scaffold," *Journal of Cranio-Maxillofacial Surgery*, vol. 31, no. 1, pp. 27–33, Feb. 2003.

[130] L.-T. Lee, P.-C. Kwan, Y.-F. Chen, and Y.-K. Wong, "Comparison of the effectiveness of autologous fibrin glue and macroporous biphasic calcium phosphate as carriers in the osteogenesis process with or without mesenchymal stem cells.," *Journal of the Chinese Medical Association : JCMA*, vol. 71, no. 2, pp. 66–73, Feb. 2008.

[131] G. A. F. Roberts, *Chitin Chemistry*. Macmillan Press, 1992.

[132] "CryoLife," 2012. [Online]. Available: www.cryolife.com.

[133] T. B. Reece, T. S. Maxey, and I. L. Kron, "A prospectus on tissue adhesives.," *American journal of surgery*, vol. 182, no. 2 Suppl, p. 40S–44S, Aug. 2001.

[134] "The Dow Chemical Company," 2012. [Online]. Available: https://dow-answer.custhelp.com/app/answers/detail/a_id/2450/~/aqucar-general-information-and-chemical-structure. [Accessed: 14-Aug-2012].

[135] P. Kilmo, A. Khalil, J. R. Slotkin, E. R. Smith, R. M. Scott, and L. Goumnerova, "Wound Complications Associated With the Use of Bovine Serum Albumin-Glutaraldehyde Surgical Adhesive in Pediatric Patients," *Neurosurgery*, vol. 60, no. 4, pp. 305–309, 2007.

[136] T. Gaberel, F. Borgey, P. Thibon, C. Lesteven, X. Lecoutour, and E. Emery, "Surgical site infection associated with the use of bovine serum albumine-glutaraldehyde surgical adhesive (BioGlue) in cranial surgery: a case-control study.," *Acta neurochirurgica*, vol. 153, no. 1, pp. 156–62; discussion 162–3, Jan. 2011.

[137] G. Hidas, a Kastin, M. Mullerad, J. Shental, B. Moskovitz, and O. Nativ, "Sutureless nephron-sparing surgery: use of albumin glutaraldehyde tissue adhesive (BioGlue).," *Urology*, vol. 67, no. 4, pp. 697–700; discussion 700, Apr. 2006.

[138] Y. Murakami, M. Yokoyama, H. Nishida, Y. Tomizawa, and H. Kurosawa, "In vivo and in vitro evaluation of gelation and hemostatic properties of a novel tissue-adhesive hydrogel containing a cross-linkable polymeric micelle.," *Journal of biomedical materials research. Part B, Applied biomaterials*, vol. 91, no. 1, pp. 102–8, Oct. 2009.

[139] G. Shi, W. Guo, S. M. Stephenson, and R. J. Lee, "Efficient intracellular drug and gene delivery using folate receptor-targeted pH-sensitive liposomes composed of cationic/anionic lipid combinations.," *Journal of controlled release : official journal of the Controlled Release Society*, vol. 80, no. 1–3, pp. 309–19, Apr. 2002.

[140] N. Li, C. Zhuang, M. Wang, X. Sun, S. Nie, and W. Pan, "Liposome coated with low molecular weight chitosan and its potential use in ocular drug delivery.," *International journal of pharmaceutics*, vol. 379, no. 1, pp. 131–8, Sep. 2009.

[141] Y. Jia, H. Joly, and A. Omri, "Liposomes as a carrier for gentamicin delivery: development and evaluation of the physicochemical properties.," *International journal of pharmaceutics*, vol. 359, no. 1–2, pp. 254–63, Jul. 2008.

[142] A. Sharma, "Liposomes in drug delivery: progress and limitations," *International Journal of Pharmaceutics*, vol. 154, pp. 123–140, 1997.

[143] C. Wiltsey, P. Kubinski, T. Christiani, K. Toomer, J. Sheehan, A. Branda, J. Kadlowec, C. Iftode, and J. Vernengo, "Characterization of Injectable Hydrogels Based on Poly(N-isopropylacrylamide)-g-chondroitin sulfate with Adhesive Properties for Nucleus Pulposus Tissue Engineering," *Journal of Materials Science: Materials in Medicine*, no. Re-submitted December 2012.

[144] S. J. Bryant, K. a. Davis-Arehart, N. Luo, R. K. Shoemaker, J. a. Arthur, and K. S. Anseth, "Synthesis and Characterization of Photopolymerized Multifunctional Hydrogels: Water-Soluble Poly(Vinyl Alcohol) and Chondroitin Sulfate Macromers for Chondrocyte Encapsulation," *Macromolecules*, vol. 37, no. 18, pp. 6726–6733, Sep. 2004.

[145] A. Jeanes and C. Wilham, "Periodate oxidation of dextran," *Journal of the American Chemical Society*, vol. 72, no. 6, pp. 2655–2657, 1950.

[146] A. Guner and I. Uraz, "Comparison of molecular association of dextran and periodate-oxidized dextran in aqueous solutions," *Carbohydrate polymers*, vol. 34, 1997.

[147] H. Zhao and N. D. Heindel, "Determination of degree of substitution of formyl groups in polyaldehyde dextran by the hydroxylamine hydrochloride method.," *Pharmaceutical research*, vol. 8, no. 3, pp. 400–2, Mar. 1991.

[148] ASTM, "F 2258-05 Standard Test Method for Strength Properties of Tissue Adhesives in Tension." pp. 1308–12, 2005.

[149] S. Burke, M. Ritter-Jones, B. Lee, and P. Messersmith, "Thermal gelation and tissue adhesion of biomimetic hydrogels," *Biomedical Materials*, vol. 2, no. 4, pp. 203–210, 2007.

[150] P. Messersmith and S. Starke, "Thermally Triggered Calcium Phosphate Formation from Calcium-Loaded Liposomes," *Chemistry of materials*, vol. 10, no. 1, pp. 117–124, 1998.

[151] W. Murphy and P. Messersmith, “Compartmental control of mineral formation: adaptation of a biomineralization strategy for biomedical use,” *Polyhedron*, vol. 19, no. 3, pp. 357–363, 2000.

[152] F. Wang, Z. Li, M. Khan, K. Tamama, P. Kuppusamy, W. R. Wagner, C. K. Sen, and J. Guan, “Injectable, rapid gelling and highly flexible hydrogel composites as growth factor and cell carriers.,” *Acta biomaterialia*, vol. 6, no. 6, pp. 1978–91, Jun. 2010.

[153] C. Brazel and N. Peppas, “Synthesis and Characterization of Thermo- and Chemomechanically Responsive Poly(N-isopropylacrylamide-co-methacrylic acid) Hydrogels,” *Macromolecules*, vol. 28, no. 24, pp. 8016–8020, 1995.

[154] L. Bian, D. Y. Zhai, E. Tous, R. Rai, R. L. Mauck, and J. a Burdick, “Enhanced MSC chondrogenesis following delivery of TGF-β3 from alginate microspheres within hyaluronic acid hydrogels in vitro and in vivo.,” *Biomaterials*, vol. 32, no. 27, pp. 6425–34, Sep. 2011.

Appendix A – Supplemental Biocompatibility Procedure and Data

A.1 – Additional Biocompatibility Procedures

A.1.1 – Live/Dead Assay

Live/Dead (LD) assays were performed to obtain a qualitative analysis of the viability of cells in each polymer mixture. The LD dye mixture was created by mixing 6.67 µL ethidium bromide (EtBr), 2.5 µL of Calcein and 5 mL of PBS in a dark or covered conical tube and the mixture was vortexed thoroughly. Control wells of PNP-CS polymer seeded with cells and cell only wells were used. As a negative control, the media above the PNP-CS polymer seeded with cells was removed and replaced with 200 µL or 70% methanol and the polymer was incubated at 37°C for 30 minutes. The media above each of the other polymer samples with and without cells and control wells was removed while the plate was heated from below to prevent phase transition. Wells were washed with 500 µL of warm PBS prior to the addition of 300 µL of LD dye mixture to each well.

Once dyed, the plate was incubated for 40-60 minutes at room temperature while covered on a shaking tray to ensure even distribution of the LD dye. Immediately prior to microscopy, an additional 10 µL of LD dye was added to each well. Cells were viewed using a fluorescence microscope with Filtersatz 15 shift adjusted, showing live cells as bright green and dead cells as red.

A.2 – Additional Biocompatibility Data

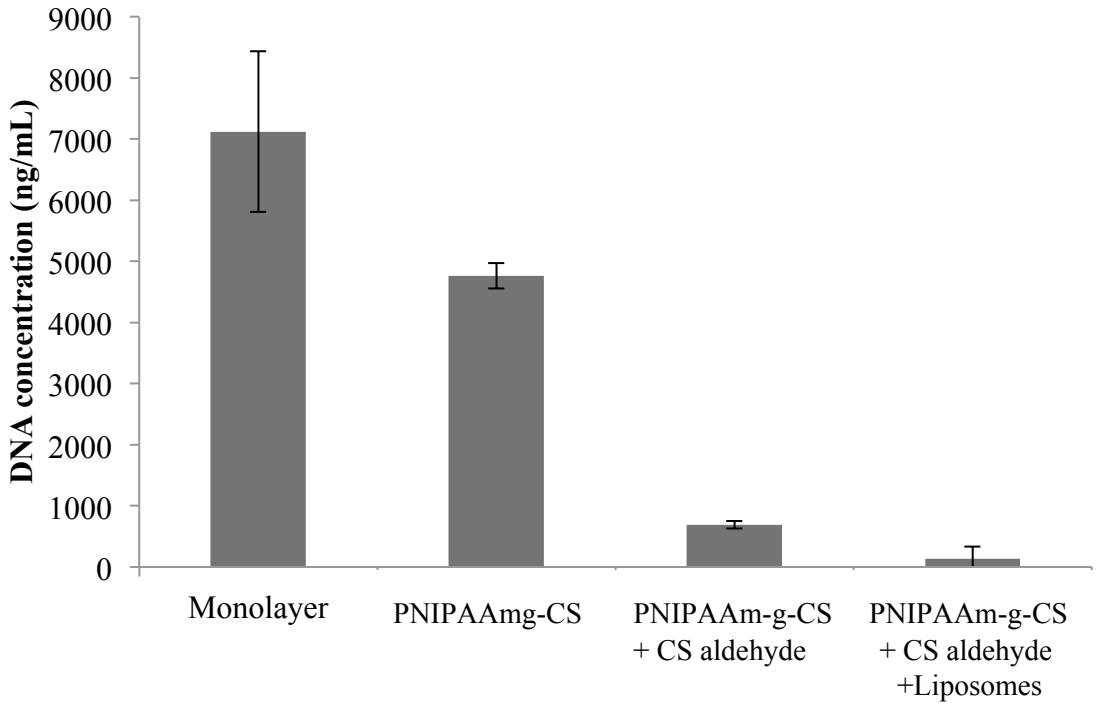

Figure 1A: Biocompatibility of polymer formulations with and without liposomes, compared with polymer only and cell only control samples using the PicoGreen Assay. Cells were seeded at 10^6 cells per mL and incubated for 5 days at 37°C (error bars represent standard deviation)

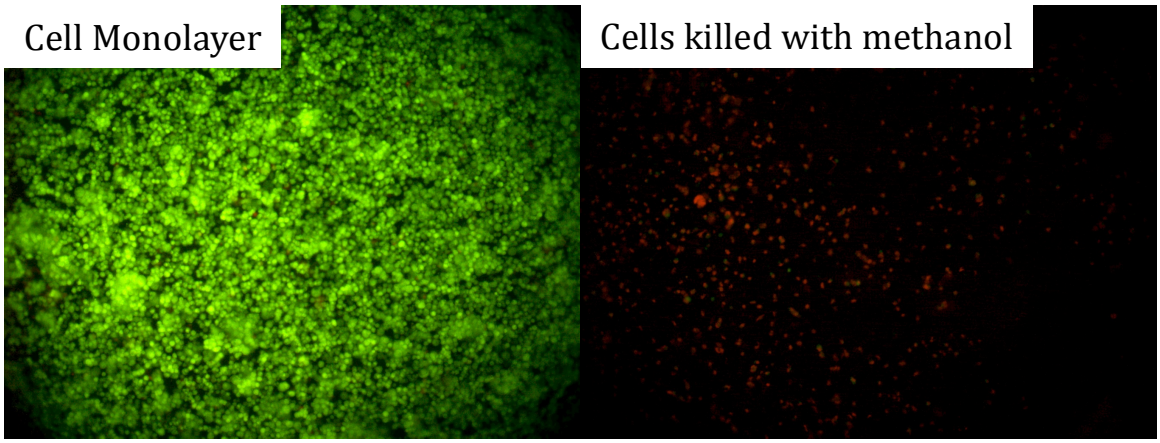

Figure 2A: Control Live/Dead wells. A cell only live well (green) and cells seeded in graft copolymer killed with methanol (red)

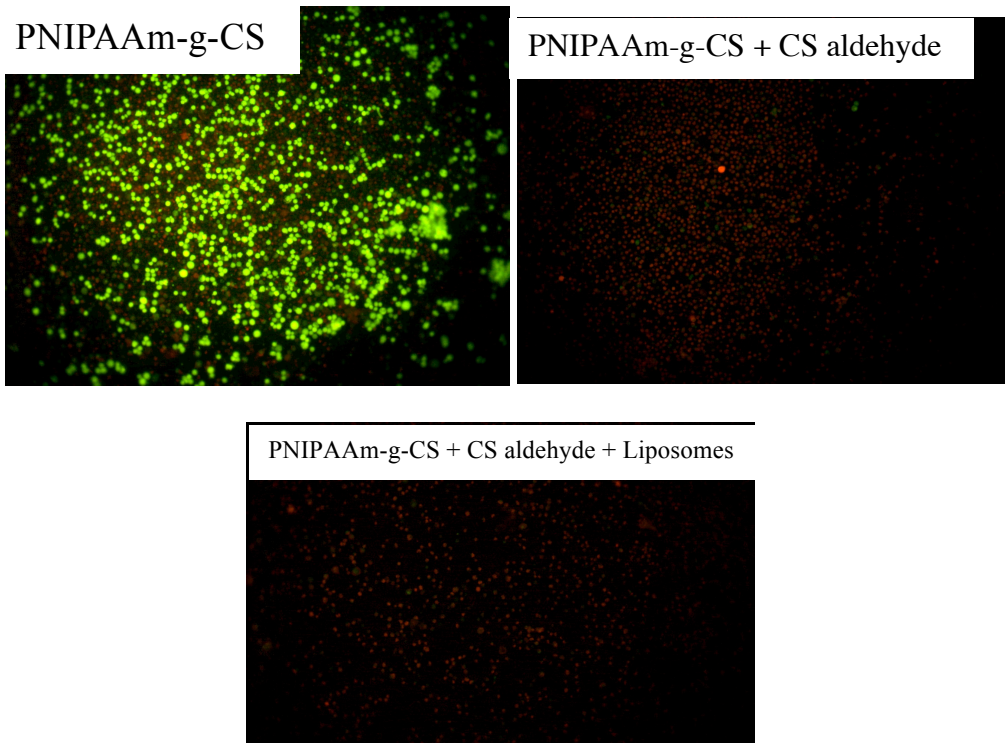

Figure 3A: Live/Dead images showing viability of cells within the copolymer alone, however dead cells in copolymer and CS aldehyde adhesive, and dead cells in copolymer, CS aldehyde adhesive and liposome blends